Title

Neural signals relating future cooperation from prisoner's dilemma feedback are outcome-contingent

Author list

Francisco Cervantes Constantino[1,*]

Santiago Garat[1]

Eliana Nicolaisen-Sobesky[1]

Valentina Paz[1]

Eduardo Martínez-Montes[2]

Dominique Kessel[3]

Álvaro Cabana[1]

Victoria B Gradin[1]

[1]Universidad de la República; [2]Centro de Neurociencias de Cuba; [3]Universidad Autónoma de Madrid

[*]Corresponding author: fcervantes@psico.edu.uy
Centro de Investigación Básica en Psicología
Facultad de Psicología
Universidad de la República
Dr. Tristán Narvaja 1674
Montevideo 11.200, Uruguay

Abstract

Cooperation upholds life in organized societies, but its neurobiological mechanisms remain unresolved. Recent theoretical analyses have contrasted cooperation by its fast versus slower modes of decision making. This raises the question of the neural timescales involved in the integration of decision-related information, and of the participating neural circuits. Using time-resolved electroencephalography (EEG) methods, we characterized relevant neural signatures of feedback processing at the iterated prisoner's dilemma (iPD), an economic task that addresses cooperation-based exchange between social

agents. We then probed the ability of relevant EEG signals to indicate subsequent decision-making, and inspected game and behavioral conditions under which they do so - including timing. Participants played against an assumed co-player, and the neural activation at the game feedback stage was analyzed via event-related potential (ERP) and spectrotemporal analysis methods. As expected from value-based decision-making studies, ERPs were increased by cooperation, including the feedback-related negativity (FRN) and the P3. In addition, we report a late potential (LP) lateralized to left frontal regions, which was also modulated by cooperation. Slow-wave, delta-band activity associated to the LP component (termed 'LP-delta') was also found to be reduced for mutual versus one-sided cooperation feedback. We then addressed individually which of these feedback signals related to subsequent cooperation and when. Crucially, the FRN, P3 and LP-delta components were modulated by choice at the next round, although involvement of each component was contingent upon the current outcome type. Immediately after one-sided cooperation ('sucker's payoff'), differential signaling indicating future decision-making occurred at the relatively early FRN, decreasing in amplitude for player choices not to cooperate at the next round. For outcomes where the player did not cooperate at the co-player expense, P3 increases were associated with subsequent cooperation by the player. Following mutual cooperation rounds, and at a relatively late stage of feedback processing, modulations by forthcoming decision were found in the form of LP-delta desynchronizations that were prospective of further cooperation. We note that the decision to cooperate in the game can be based on predicting different aspects of the prospective interaction given the past realized outcome (e.g. whether 'to sustain' mutual cooperation or 'to retaliate' if it is one-sided). The results support information integration for cooperation decision-making at the iPD, beginning at different timescales and circuits, by such updating context. The specific case of verifying a partner's cooperation entailed a shorter reciprocation response which was predictable by feedback signal changes at the immediately preceding

trial. A neurally informed account of fast-mode dual-process mechanisms, and involvement of predictive coding principles in guiding cooperation with a partner at the iPD, are discussed.

Keywords

FRN

P3

delta

frontal asymmetry

social interaction

social heuristics

cooperation

game theory

prisoner's dilemma

EEG

Highlights

*FRN, P3 and late delta-band asymmetric frontal activity encode cooperation feedback

*Decision to cooperate in iterated prisoner's dilemma indicated by prior round signals

*Speed of reciprocating partner's cooperation correlates with single-trial activity

Introduction

Engaging what is best individually and collectively is a hallmark of cooperation in groups. The intuition that benefits may increase exceedingly when sought by mutual cooperation[1] is embodied in the iterated prisoner's dilemma (iPD) game, which addresses strategic interactions between agents in

trust-based settings[2,3]. The goal of this iconic game is for participants to maximize earnings by making simultaneous and independent decisions on whether to cooperate with each other, mutually affecting each other's outcomes. Feedback on both players' decisions is learned at the end of each iteration, where participants may retain the ability to adopt cooperation strategies at later rounds. The iPD has been used to gain understanding into the organization and function of brain systems in neuroeconomics and social neuroscience[4–13], as well as for applications of clinical interest[14–21].

High temporal resolution electroencephalography (EEG) methods are well-suited to characterize the timecourse of cooperative decision-making. For the iPD, such studies have primarily relied on dyadic measures from hyperscanning methods[22–24], addressing strategic choice during partner gameplay and associations with inter-subject functional connectivity patterns. Of a relatively simpler scope, event-related potential (ERP) and spectrotemporal analysis are nevertheless prominent techniques to infer the neural bases and timing of economic decision-making[25]. Their application to the iPD has been relatively scarce[26,27], including only one ERP study of the early (i.e. <600 ms) feedback stage. We aimed first for a comprehensive characterization of the feedback processing stage of the iPD extending to its late stages and spectrotemporal activity which, to the best of our knowledge, have not been addressed before. Secondly, we took into consideration that a key goal for studies of cooperative decision-making is to predict forthcoming choice as early as possible. It has been noted that the game feedback stage may provide with an important analysis window to predict cooperation[28]. For instance, in a study of the iPD the P3 feedback component was associated to belief updates about the co-player's willingness to cooperate in the next trial[27]. We hypothesized that in the iPD, time-resolved neural signatures of cooperative decision-making at the next round may be observed as early as during feedback processing of the previous round. Therefore, we evaluated whether ERP and spectrotemporal signals identified at the feedback processing stage were indicative of subsequent cooperative behaviour.

Value-based feedback ERP components relevant to the iPD

Among ERPs in *value-based decision making* studies, the first stage of (visual) feedback processing is represented by the N1, an occipital bilateral complex indicating early cortical perceptual processing[29]. It is often followed by the feedback-related negativity (FRN), a difference waveform interpreted as the first learning stage in outcome processing[25]. Its dependency on reward valence, magnitude and expectancy has served to interpret it as a prediction error signal in the reinforcement learning framework[30–34]. The FRN primarily reflects reproducible differences between optimal and worst reward outcomes, and may be weaker relative to ongoing background P3 activity[35]. Careful consideration is thus required in FRN estimation as different approaches may lead to inconsistent effects[36] (see[25,33] for a review). The P3 (or alternatively, the P3b subcomponent) is a widely studied ERP from the *perceptual decision-making* literature, with centro-parietal and/or temporo-parietal scalp distributions[37–42]. It is considered to represent probabilistic stimulus updating[43–45] in working memory for event categorization[38]. It has also been interpreted as an index of the rate or endpoint at which evidence converges towards a decision[46,47], hypothesized to facilitate decision-making by optimizing signal conduction across relevant networks[39,48]. In value-based decision making, the P3 is part of feedback processing[25,27,49], and shows sensitivity to reward magnitude, valence and probability/risk[50–58]. As in perceptual studies, the feedback P3 may reflect update and storage of reward values for behavioral adjustment[25,59–62], by integrating them with internal models of a probabilistic task[63]. It may similarly reflect reward evidence accumulation dynamics[64], possibly as a decision variable for strategic choice[65]. The P3 has been shown to be enhanced with mutual cooperation at the iPD, associated with evidence buildup of trust beliefs between interacting partners[27]. For a thorough analysis of time-resolved neural signatures of cooperation at the iPD, we first studied the N1, FRN and P3 signals, but also late-latency,

and spectrotemporal activity associated to each of these ERPs. At the next part of the study, we investigated all relevant feedback signals (i.e., found to be modulated by cooperation choices leading to the present outcome) for their potential to indicate subsequent cooperation[66].

ERP analyses by forthcoming choice: timing and dual-access theories

The timecourse of decision-making is addressed in dual-process theories[67,68], which account for two alternative processes that lead to the same outcome but over different time frames. With regards to cooperation, these models have emphasized the faster decision to collaborate by default, versus the slower decision to consider 'second thoughts' of self-interested nature[69–71]. It is unclear however how are 'fast' versus 'slow' decisions implemented neurally, and at which timescales. We specifically refer to the time interval spanning between last feedback presentation and subsequent response, which plausibly, contains the full decisional process for that iteration - from updating to execution. Here, we considered critical domains overlapping the encoding of *prior choice* that led to the current context, and the encoding of *subsequent choice*. For that reason we performed a comprehensive search of relevant update processes for their potential to relate to the next decision making. Given the relatively limited ERP literature on iPD feedback processing, information about the timing of scalp activity components involved in decision processes following each outcome also remains unclear. It is important to note that each outcome type sets a distinct context at the iPD: for instance, if cooperation turns out to be mutual at the present round, the subsequent decision may be framed in terms of whether to sustain cooperation further; otherwise, the decision may be primarily about retaliation. To control for such potential differences, once relevant feedback components were determined, we conducted an independent search of their activity in correspondence to each outcome, and partitioned trials on the basis of whether they led or not to cooperation at the following trial. Once the feedback components

that were *also* involved in subsequent choice were identified, we addressed their key timing information and potential association to faster versus slower modes of decision-making.

Methods

Subjects.

Thirty-one volunteers (16 female; mean age 22.3 ± 2.9 SD) with no history of neurological or psychiatric disorders participated in the present study voluntarily after providing informed consent. Participants were enrolled in academic degree programs in the Uruguay tertiary education system, or had completed them. They reported normal or corrected to normal visual acuity. All experiments were performed in accordance with WMA Declaration of Helsinki guidelines. The Ethics in Research Committee of the Faculty of Psychology at Universidad de la República approved the experimental procedures. Prior to attending the experimental session, participants completed an online questionnaire on social behavior (Inventory of Interpersonal Problems, Horowitz et al 1988). These data were not used in the present study. The first half of one subject's session data were not recorded, but the remainder (100 trials) were included in the present analysis.

Experimental setup

Visual presentation and response time logging were performed with custom PsychoPy[72] software at the Centro de Investigación Básica en Psicología (CIBPsi) EEG lab. Displays were delivered over a CRT monitor (E. Systems, Inc., CA) with 40 cm size, 83 dpi resolution, and 60 Hz refresh rate. Continuous EEG recordings were performed using a BioSemi ActiveTwo 64-channel system (BioSemi, The

Netherlands) with 10/20 layout, at 2048 Hz digitization rate with CMS/DRL (ground) and two mastoid reference electrodes, the average of which was removed offline from the rest of channels. A 5th order cascaded integrator-comb low-pass filter with -3 dB point at 410 Hz was applied online, after which the signals were decimated to 256 samples per second. Electrooculographic data were recorded supra- and infra-orbitally as well as from the left versus right orbital rim. Data were acquired at 24 bit resolution and analysis was performed offline. Full experimental sessions lasted ~2.5 h.

Experimental protocol

Each participant was introduced to a same-sex person presented as their co-player for the study, but which in fact was a confederate. The assumed co-player was then escorted to a separate location, and the participant proceeded to the main experimental facility. The iterated prisoner's dilemma (iPD) task was explained to the participant, who was told that on each trial both players would have to make a simultaneous and independent decision regarding whether to cooperate or not cooperate with each other. Depending on their decisions they would both receive points on each round. Mutual cooperation ('CC') [non-cooperation ('DD')] earned both players 2 [1] points respectively, while unbalanced outcome types ('CD' and 'DC') earned 0 points for the player that cooperated and 3 for the player that did not. Participants were familiarized with the outcome abbreviations. They were told that his/her points, and those of the other player, would be accumulated at the end of the game and that they would be paid as a function of the final result. After this, the participant did a practice test to demonstrate task comprehension. A pause was made so as to pretend providing identical instructions to the co-player at the separate room. During recordings, participants played the iPD over a visual

interface (14.4° wide by 6.2° high) representing online gameplay with their assumed co-player, simulated in fact by a probabilistic algorithm (see below), and were instructed to maximize earnings. In each round of the iPD, the participant is presented with 'Cooperate' ('Cooperar', in Spanish) or 'Not cooperate' ('No cooperar') choices with respect to their co-player. After an initial visual fixation period (uniformly distributed between 1–2 s), the game payoff matrix was displayed (Figure 1A) and participants were required to make a decision by pressing one of two buttons (left/right), which would then highlight the corresponding column of the payoff matrix. Left/right selection was randomized along with column display order across trials. After a second wait and fixation period (ranging 1.75 – 2 s), the joint final outcome was highlighted as feedback. In each round, the type of outcome was determined by the joint decision of the player and the virtual co-player, and resulting gains were accumulated over iterations. Decision-making by the assumed co-player was simulated by a probabilistic 'tit-for-tat' style algorithm. In the first round, the algorithm cooperates and in rounds thereafter it reciprocates the player's previous choice with 80% probability. However, given three consecutive rounds of identically-balanced joint outcomes (i.e. mutual [non]cooperation), the algorithm will switch opposite at the subsequent round. An optional pause with ad lib duration was made every 50 rounds. Participants completed 200 rounds of the game.

After the experiment, each participant completed 8-level subjective Likert rating scales on the emotional response (happiness, anger, sadness, betrayal, and guilt) to each of the four different outcomes of the iPD. A subset of 26 participants additionally completed 5-level subjective Likert rating scales on dominance[73,74] and intrasexual competition[75]; these data were not analyzed in the present study. At the end of the session, participants were debriefed regarding the co-player, and no one reported any distress about the cover story. Data from one participant that did not believe the

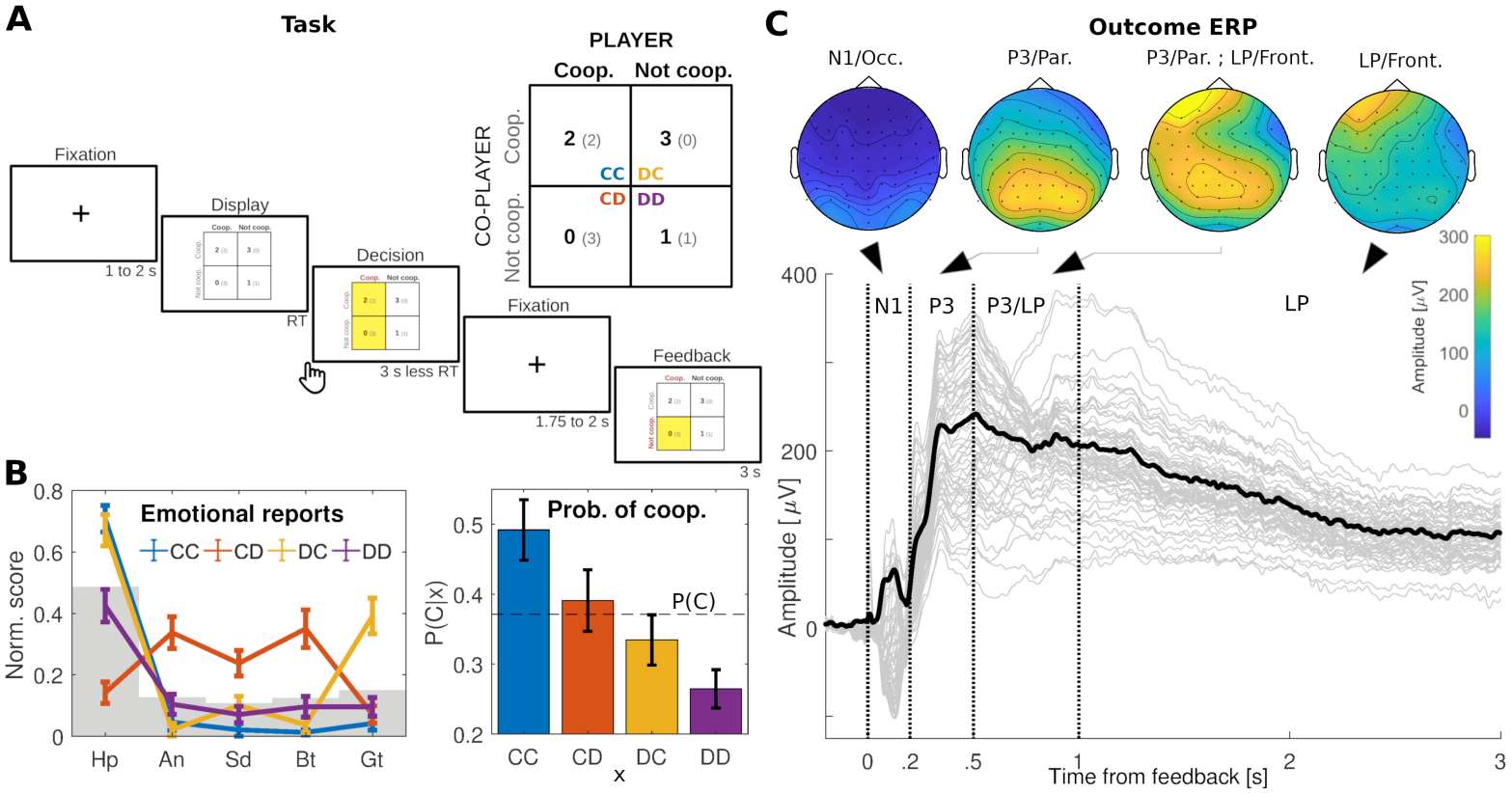

Figure 1. Presentation of the iPD and associated emotional, behavioral and neural variables. (A) Visual display of the task. The game matrix (inset) assigns earnings to both players as a joint function of their decisions to cooperate with each other. The resulting combinations apportion different amounts to player vs co-player earnings (indicated in large vs small fonts respectively). CC: mutual cooperation; DD: mutual non-cooperation/defection; CD: one-sided cooperation/'sucker's payoff'; DC: one-sided defection). At each trial, the matrix is displayed after a fixation period, prompting for the participant's decision. When made, two possible outcomes given his/her choice are briefly highlighted. After a second wait period, the final outcome is indicated. (B) Left: across participants (N=30), each of the game's outcome leads to a distinct emotional profile (Hp: happiness; An: anger; Sd: sadness; Bt: betrayal; Gt: guilt), where both CC and DC gain outcomes may be associated with happiness/satisfaction emotions but only the latter carries on additional guilt reports. CD may be associated with mostly negative emotions (see Results). Grey level indicates outcome report averages by emotion. Right: the probability to cooperate after a trial is influenced by the involved decisions in the present trial; dashed line indicates average baseline levels. Error bars indicate ±1 SEM. (C) In the EEG, the feedback stage of the iPD consists in average of a progression of components. Initial occipital N1 activity peaks around 100 ms, followed by a fast-rising parietal P3 component which vanishes until about 1 s. Transition into a frontal, left-lateralized late potential (LP) begins at about 500 ms, and is

sustained until the end of the trial (Supplemental Video). Topographies indicate time averages over the selected windows. Black line indicates root-mean-square over channel data (grey).

cover story were removed from analysis. Thus, the final sample for analyses included 30 subjects. Participants received a cinema ticket in appreciation for their time.

Data analysis

Questionnaire and behavioral data

In order to address ecological validity of the game, participants rated emotional reactions to each of the iPD outcomes at the end of the session. First, emotional responses from questionnaire ratings were normalized from 0 (emotion 'not at all' experienced) to 1 ('experienced extremely'), and were specific to each outcome type. Second, the participant's probability of cooperation at any trial was estimated as a function of the last outcome type. This allowed probing whether participants may adapt their cooperation strategy with regards to self and co-player choices. Finally, reaction times were computed as the interval between game payoff matrix presentation onset, and player button press at each trial. For single-trial analyses of reaction time (see below), data from the first trial and trials beginning after pause were not considered.

Statistical analyses for emotional and behavioral data

Emotional ratings were analysed using a two-way ANOVA with factors emotion and outcome types.

An ANOVA with factors Player and Co-player choice was used to analyse the probability of cooperation. Reaction times were analyzed similarly. On a separate analysis of reaction time, we compared the time taken to elect to cooperate versus not cooperate.

EEG processing

EEG data were re-referenced to the average of the left and right mastoid channels, after which DC offset was removed from each channel, to be bandpass-filtered in the 0.1 – 30 Hz region with a fourth-order Butterworth filter in the forward and reverse direction. Trials were epoched in the -0.25 to 3 s interval of feedback presentation onset. Single channel data were subsequently rejected according to a variance-based criterion[76] applied over the 2-D matrix of time (3.25 s) by channel-epochs (64 sensors by 200 trials = 12800 timeseries), with confidence coefficient $\lambda_P = 4$ in a blind manner. This resulted in removal of 0.7 ± 0.4 % (mean ± SD) of all data across 30 participants (see resulting distributions of data per outcome type, below). To address variability across participants, which can affect the spatial filtering method (see below), the blind rejection procedure was repeated over the collated 2-D matrix of timeseries across participants (up to 12800 timeseries by 30 subjects). This resulted in 1.75% rejected single-channel trial timeseries across the experiment, including the data already removed (subject range 0.1% - 13.9%).

ERPs and spatial filtering

ERP components, specifically their associated temporal windows and spatial topographies, were selected from inspection of all ERP spatiotemporal profiles present during iPD feedback processing.

For this, first, all epochs were averaged across all conditions and participants regardless of outcome (Supplemental video 1), as a general feedback grand average. Second, a sequence of components associated with the N1, P3 and a frontal left-lateralized late potential ('LP') was directly observed in this grand average by distinctive occipital, parietal, and left-frontal spatial distributions respectively. Each spatial distribution was then inspected for the temporal window in which it was uniquely featured in the grand average. This resulted in three interval windows of interest, N1: 0 – 0.2 s, P3: 0.2 – 0.5 s, and LP: 1 – 2.5 s. Estimation of ERP components is known to be sensitive to experimenter selection of a sensor or sensor cluster[25] where the signal of interest is hypothesized to be found. To address this issue, we introduce an application of spatial filtering methods that estimates selection coefficients for these components, principled on the component's reproducibility across trials and participants[35]. In the classic approach, ERPs are analyzed in a subset of sensors selected by the experimenter according to the hypothesis of its optimal spatial location. This implies that scalp data are effectively factored by sensor weights (e.g. 1 for the target channel and 0 elsewhere). To derive such values in a data-driven manner and to improve signal-to-noise ratio compared to sensor selection, a 'joint decorrelation' (alternatively, 'denoising by spatial separation') procedure was implemented for spatial filtering[35,77,78]. This was first designed to estimate sensor weights representing each of the three evoked spatial profiles of interest, separately, as observed in scalp EEG dynamics during feedback processing. This consisted of extracting a linear combination of sensor coefficients that yields, within each window, the most reproducible spatial activity profile across trials and participants after weighted averaging. To prevent extraction of residual variation not representing the average, and considering the relatively shorter windows (e.g. 0.2 s), the baseline period was pre-concatenated to every window before training. This resulted in a set of three (non-orthogonal) linear combinations

(Supplemental Figure 1A). In other words, the original 64-channel ERP dataset was mapped to three components that, separately, optimize detection of evoked activity within each time interval. The associated sensor weights remained fixed across participants, conditions, and time. The three relevant N1, P3 and LP spatial profiles originally observed in the evoked signal were thus recovered from the resulting spatial filter coefficients (Supplemental Figure 1B,C).

Afterwards, in order to also obtain the feedback-related negativity (FRN) ERP from reward processing studies[30,50,79], we selected the P3 temporal window from which the relatively weaker FRN signal may be extracted, for sensor weight estimation via joint decorrelation. For this, the bias criterion[35] was changed to exploit the reproducible differences between iPD mutual cooperation (CC) and unreciprocated cooperation (CD) outcomes. The resulting linear combination maximized the separation between these two outcome conditions, reproducibly across subjects, revealing a spatial topography associated to the FRN[36] (see Discussion).

Finally, to prevent residual contamination effects as a result of ERP low signal-to-noise ratio driving subsequent analyses, only data from the subset of 26 participants that attained a minimum of 10 repeats of each outcome were further analyzed (CC: 42 ± 21; CD: 38 ± 13; DC: 49 ± 11; DD: 64 ± 24 trials across participants).

Spectrotemporal analysis.

Involvement of differential rhythmic activity profiles at the iPD feedback processing stage was addressed. To this end, time-frequency evoked power measures were obtained from spectrotemporal

maps (correlograms) in the 1 – 25 Hz spectral region via the continuous Morlet wavelet transform, log-transformed to a dB scale with average baseline values as reference. This procedure corresponds to the event-related spectral perturbation[80,81] estimate of the ERP. Maps were separately analyzed on each of the four components of interest, N1, FRN, P3 and LP, and within each component's window, as featured or estimated in the ERP overall (N1: 0 – 0.2 s ; P3: 0.2 – 1 s ; LP: 0.5 – 2.5 s ; FRN: 0.2 – 0.5 s) (note that these *presence* windows may differ from those used for spatial filter *estimation*). Due to the baseline referencing involved, and to prevent systematic pre-causal differences as a result of foreknowledge of the player's executed choice immediately prior to feedback, spectrotemporal contrast analyses[82] were performed only between condition pairs with a common prior action by the player, namely 'CC' versus 'CD', and 'DC' versus 'DD'.

EEG statistical analysis

The first part of the study contains analyses related to *current outcome choices*, where feedback data were probed by the separate decisions that the player and the coplayer made leading to the present outcome. The second part of the study relates *next choice* analyses, where relevant feedback signals were contrasted by the forthcoming decision to cooperate that the player is to make at the subsequent round. Unless so indicated, statistical analyses were performed with MATLAB® (The Mathworks, Natick, MA).

Current outcome choices

ERP analysis. Participants' datasets converted to relevant N1, FRN, P3, and LP component subspaces by spatial filtering (Supplemental Figure 1C) were averaged across the corresponding temporal window in which the underlying evoked component was observed to be present, as indicated above.

General feedback components (i.e. N1, P3 and LP) were tested for modulations by choices made by each player on the current trial. Data were submitted to a 2-way repeated measures ANOVA, in order to test how Player and Co-player decisions' had a modulatory effect on each feedback processing stage.

Spectrotemporal cluster analysis. Cluster regions relevant to outcome processing were obtained by estimation of the *t*-value map from condition contrasts (i.e. CC vs CD, and DC vs DD). An a priori threshold of *t*=2 (corresponding to the distribution 97.5 percentile approximately) was used for non-parametric randomization-based statistical testing[82,83]. A cluster was deemed significant if its associated *t*-statistic (sum of *t*-values within the cluster) exceeded those within the randomization distribution at an α=0.05 level of significance. The distribution was generated by *N*=1024 resamplings of the original experiment, where for each resampling, conditions involved in the contrast (e.g. 'CC' and 'CD') were randomly shuffled per participant prior to establishing the contrast of the grand-averages. After cluster identification, measures for posterior analyses were obtained by double integration across the time and frequency within relevant cluster boundaries. Prior to integration in the spectral domain, scaling compression bias due to logarithmic-spacing of frequency was prevented, by converting the distribution of time-integrated marginals over frequency to linear scale.

Next choice

ERP and spectrotemporal cluster analysis. Critically, once relevant outcome processing modulations were identified, the signals were re-tested for the hypothesis that they may relate to the participant's decision at the next round. In each case and for each outcome, single trial data were partitioned by whether, at the next round, the player would go on to cooperate or instead chose to defect (e.g. 'C|

CD' versus 'D|CD'). Being of identical economic value, such contrasts may reveal differences that, during outcome processing, may be directly involved in decision-making. As before, data from participants that attained a minimum of 10 repeats per sub-condition (n=16 for C,D|CC; n=18 for C,D|CD; n=21 for C,D|DC) were analyzed, independently for each relevant component (e.g. FRN, P3, LP, LP-cluster) found in prior analyses. Trial data partitioned by next decision were tested for normality by Shapiro-Wilk tests implemented with SPSS Statistics 24 (IBM Corporation, Armonk NY), and submitted to Student's t, or alternatively to Wilcoxon rank-sum testing as applicable, corrected for multiple comparisons.

Since the number of trials within partitioned conditions were imbalanced, to discard the possibility that observed effects may be attributable to relative signal-to-noise fluctuations in the evoked signal (reflecting upon different sample sizes), additional non-parametric randomization tests were performed. The distribution consisted of 2^{15} resamplings where for each participant, trial data were randomly shuffled across 'subsequent-decision' conditions, while maintaining the original sample sizes. For each resampled version of the experiment, an effect size was computed by trial-averaging per nominal condition, followed by grand-averaging across subjects. The difference between conditions represented that resampling effect size. Empirical effect sizes were then compared against those from the resampled distribution, and significance assessed by one-sided testing of the hypothesis of no difference between subsequent decisions[84].

EEG and reaction time correlations. EEG signals that were found to be indicative of next choice at the previous analysis were then examined at the single trial level for their association to forthcoming reaction times. Single trial data across the experiment (26 subjects) were submitted to repeated measures Pearson correlation analysis[85] performed to test the strength of the linear association

between EEG and reaction time variables, accounting for non-independence of trial-based measures at the within-subject level. This was implemented with RStudio, version 1.2.1335 (RStudio, Inc., Boston, MA).

RESULTS

Emotional and behavioral results

The iPD (Fig 1A) triggers distinct emotions and behavior according to the type of outcome received as feedback. A 2-way repeated measures ANOVA on emotional reported scores identified significant main effects for emotion type ($F(4,116)=68.1$; $p<0.001$; $\eta_p^2=0.701$), outcome type ($F(3,87)=9.8$; $p<0.001$; $\eta_p^2=0.252$), and a significant emotion by outcome interaction ($F(12,348)=29.6$; $p<0.001$; $\eta_p^2=0.505$). Follow-up analyses included independent ANOVAs per emotion type, with outcome type as factor. Each outcome type was associated with specific emotional reactions (Fig 1B), consistent with previous work[14,21]. Specifically, CC outcomes were associated with feelings of happiness; CD outcomes with anger, sadness and betrayal; DC outcomes with satisfaction and guilt; and DD outcomes with intermediate levels of these emotions (Supplementary Table 1; Fig 1B).

Behaviorally, transition probabilities, (i.e. the probability that the player will cooperate at a next trial given the type of outcome in the present trial) were analyzed. A 2 x 2 factorial repeated measures ANOVA was run with Player and Co-player choices (i.e. C versus D each) as independent within-subjects variables. A significant main effect of Player choice on subsequent probability to cooperate was found ($F(1,29)=24.7$; $p<0.001$; $\eta_p^2=0.460$), where cooperation by the Player led to higher chances of cooperating in the next round. Similarly, a significant main effect of Co-player choice was found ($F(1,29)=17.4$; $p<0.001$; $\eta_p^2=0.376$), where cooperation led to a higher probability that the participant will cooperate in the next round. The interaction between Player and Co-player choices on transition

probability was not significant ($F(1,29)=0.52$; $p=0.48$; $\eta_p^2=0.02$). Data from a participant with near-zero cooperation rates were removed from subsequent analyses.

Reaction times were examined with a similar 2 x 2 design as above, and a significant main effect of Player choice on subsequent reaction time was found ($F(1,28)=5.64$; $p=0.025$; $\eta_p^2=0.168$) (Supplementary Figure 2A). No significant effect by Co-player choice was found ($F(1,28)=1.84$; $p=0.19$; $\eta_p^2=0.06$). The main effect of Player choice was qualified by a significant interaction between Player and Co-player choices over subsequent reaction times ($F(1,28)=4.44$; $p=0.044$; $\eta_p^2=0.14$). Post-hoc comparisons indicated that reaction times at the next round were on average 77 ms faster (CI: 28 to 125 ms; Cohen's $d=0.6$) if both Co-Player and Player cooperated than if only the Co-Player did ($t(28)=3.23$; $p=0.003$), i.e., after CC versus DC outcomes (Supplementary Figure 2A). By contrast, given non-cooperation by the Co-player, subsequent reaction times did not significantly differ regardless of any choice made by the Player ($t(28)=0.06$; $p=0.95$). Finally, when all trials were pooled and analyzed for the reaction time to make a decision to cooperate or not (see Methods), a nonsignificant trend was found in the differences taken to cooperate (880 ± 173 ms; mean ± SD) and to defect (946 ± 197 ms) ($t(28)=2.000$; $p=0.056$).

EEG outcome results

As explained above, across outcomes, and subjects, visual feedback at the iPD triggers a sequence of event-related potentials (ERP), shown by an evoked grand-average that includes early occipital N1, mid-latency parietal P3 and a sustained left-lateralized frontal, late potential ('LP') (Fig. 1C, Supplementary Video 1). A spatial filtering technique to improve signal-to-noise ratio in evoked neural activity[77], *joint decorrelation*[35,78], was applied to feedback epochs across trials and subjects. This extracted reproducible component waveforms corresponding to the N1, P3 and LP ERP distributions as evoked during feedback processing (Supplementary Figure 1). After projection to component space,

data were separated by outcome condition and analyzed for modulations effected by *current outcome choices*. Finally, the feedback-related negativity (FRN), which represents difference waveform activity, specific to an outcome contrast[25], was extracted via an adapted application of joint decorrelation[35].

N1

Figure 2A shows that N1 component waveforms appear to be similar regardless of outcome type. Mean amplitude data from this component at the 0-0.2 s interval were submitted to a 2 x 2 repeated measures ANOVA with *current outcome choices* by the Player and Co-player as factors, showing no significant main effect of either (Player: $F(1,25)=3.45$; $p=0.075$; $\eta_p^2=0.121$; Co-player: $F(1,25)=0.09$; $p=0.77$; $\eta_p^2=0.004$) or interaction ($F(1,25)=1.13$; $p=0.30$; $\eta_p^2=0.04$) (Fig. 2B).

P3

Waveforms from P3 component were equally tested for effects related to *current outcome choices* (Fig. 2A). Since visual inspection of the grand-averaged ERPs (across outcome types) indicated that this component distribution may be present over the 0.2 – 1 s interval post feedback onset (Fig. 1C, Supplementary Video 1), amplitude data for analysis was averaged in this time window. A significant main effect of Player choice was found ($F(1,25)=9.74$; $p=0.005$; $\eta_p^2=0.28$), as well as a significant main effect of Co-player choice ($F(1,25)=11.94$; $p=0.002$; $\eta_p^2=0.32$), but no significant interaction ($F(1,25)=0.95$; $p=0.34$; $\eta_p^2=0.04$). For each main effect the choice to cooperate (by the Player or Co-player) led to greater waveform amplitudes (Fig 2B).

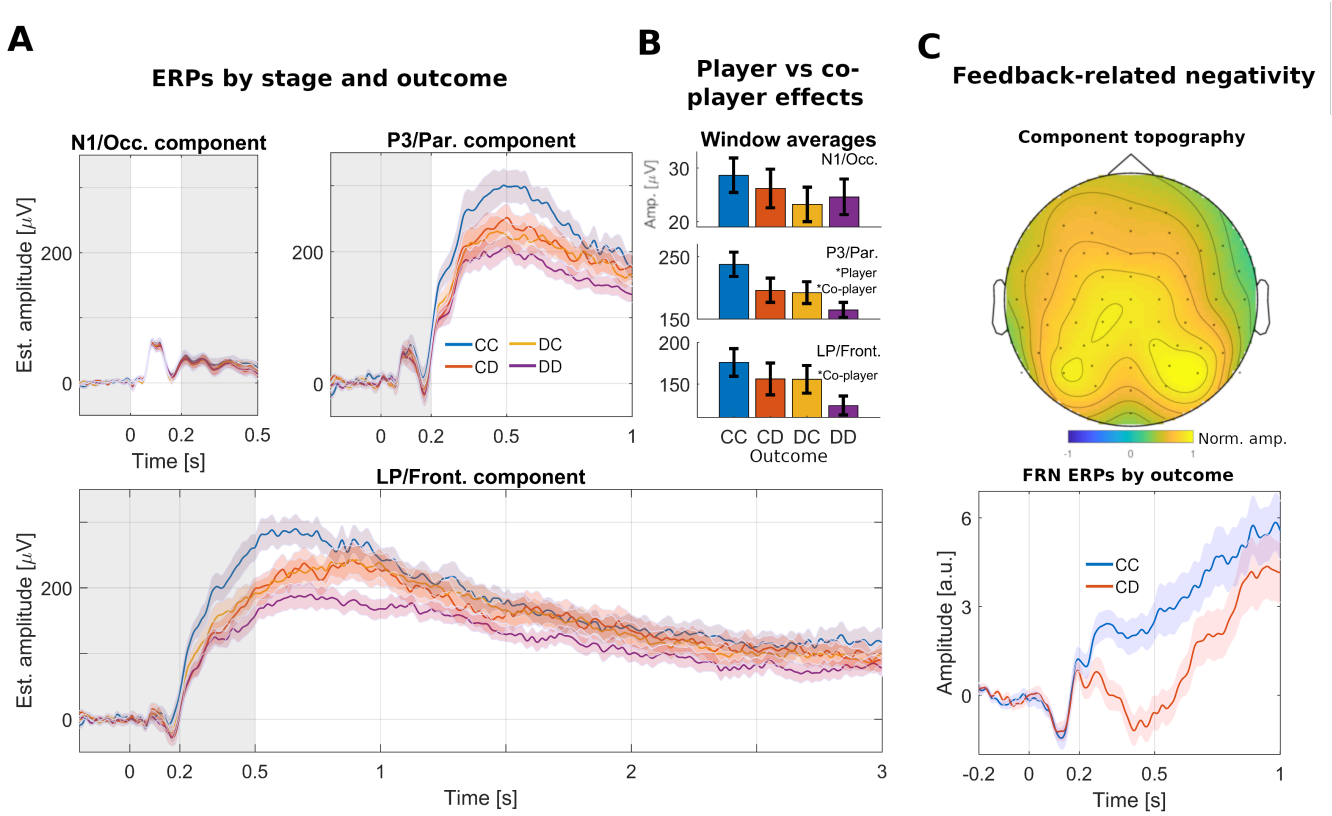

Figure 2. Component-specific processing of player and coplayer choices during iPD feedback. (A) General feedback components N1, P3 and LP were estimated via spatial filtering (Supplemental Figure 1). Top left: The visual N1 (0-200 ms; non-shaded region) shows no effects of outcome processing related to players' choices. Top right: The P3 is the first general feedback component where effects of player and coplayer choices are observed, without interaction, over the 0.2-1 s window. Bottom: Analyzed over the 0.5-3 s interval, the LP shows an effect of co-player's choice. Curve shades indicate ±1 SEM. (B) Summary of window averages and effects found for all relevant stages and outcomes. (C) The outcome-specific feedback component FRN was separately extracted from reproducible scalp activity which differentiates between cooperation reward outcomes (CC versus CD) across participants, also by spatial filtering. Top: the component centro-parietal topography. Bottom: its timeseries at the 200-500 ms window shows sensitivity to co-player's choice given cooperation by the participant.

LP

The LP component was the final stage where *current outcome choice* differences were observed in associated waveforms (Fig. 2A). Mean amplitude data were computed over the 0.5 – 3 s interval where

component presence was indicated in the grand-averaged ERP across outcome types (Fig. 1C, Supplementary video 1). Statistical analysis revealed no significant main effect of Player choice ($F(1,25)=3.36$; $p=0.079$; $\eta_p^2=0.12$), a significant main effect of Co-player choice ($F(1,25)=4.68$; $p=0.040$; $\eta_p^2=0.16$), and no significant interaction ($F(1,25)=0.38$; $p=0.55$; $\eta_p^2=0.02$). As before, Co-player choice to cooperate led to higher amplitudes on average (Fig 2B).

FRN

Unlike the previous components the FRN represents differential, outcome-specific activity of feedback processing[25,33,36]. For a spatial filtering implementation, this component was extracted by a modified two-stage joint decorrelation[35] procedure based on the early P3 epoch subspace (0.2 to 0.5 s, see Methods), serving to address relatively weaker sources in evoked differences between conditions. As result, a linear combination of sensors was obtained representing a scalp profile that reproducibly distinguishes between CC and CD outcomes across trials and subjects. This component displayed a centroparietal scalp topography (Figure 2C). We confirmed a significant difference in the mean amplitude of associated waveforms between CC (2.0 ± 2.1 a.u.; mean ± SD) and CD (-0.2 ± 2.1) conditions ($t(25)=5.55$; $p<0.001$; Cohen's $d=1.09$) over the corresponding 0.2-0.5 s interval (Figure 2C).

Time-frequency analysis

Spectrotemporal analyses were performed to parse modulations by feedback processing not directly reflected on the waveform. Non-parametric spectrotemporal cluster analysis methods[82,83] were applied to address differential modulations in evoked signal power by outcome for each ERP within its corresponding temporal window. Due to potential baseline differences as a result of player's knowledge

of her/his own choice, contrasts were limited to conditions that may be assumed as identical up to the time of feedback - namely CC versus CD, and DC versus DD outcomes.

For the N1, FRN and P3 components, no significant gain variations in evoked power were found in either contrast. However, inspection of the evoked power measures from LP signals indicated late and sustained suppression of slow-wave activity (<5 Hz) which was modulated across outcomes (Figure 3A). For the CC versus CD contrast (feedback after player cooperating in the current outcome), statistically significant gain variations were found for a spectrotemporal cluster in the lower delta region (median: 1.34 Hz; half maximum 1.1–1.7 Hz) at the 0.57–2.18 s time range (p=0.002), and for a second cluster in the higher delta band (median: 3.25 Hz; half maximum 2.6–3.7 Hz) at the 1.62–2.51 s time range (p=0.034). This was due to evoked power demodulation, relative to baseline, within the delta band at left frontal scalp regions for mutual versus unreciprocated cooperation outcomes. No statistically significant spectrotemporal clusters from the LP component were found in the DC versus DD contrast.

Outcome processing modulations by subsequent decision

The FRN, P3, and LP waveforms, as well as the spectrotemporal clusters associated to the latter, were next addressed in their potential to indicate participants' *next choice* to cooperate. For this analysis, for each outcome, trials were also partitioned by the player's decision at the subsequent round. For example, following CC outcomes, participants may either cooperate ('C|CC') or not ('D|CC').

Mutual cooperation. Significant modulations by *next choice* were not found in waveform activity after mutual cooperation, as shown by one-sample t-tests or, where applicable, Wilcoxon rank-sum tests, for the FRN (t(15)=0.62; p=0.54; Cohen's d=0.16), P3 (t(15)=0.94; p=0.36; d=0.24), nor LP (t(15)=1.48;

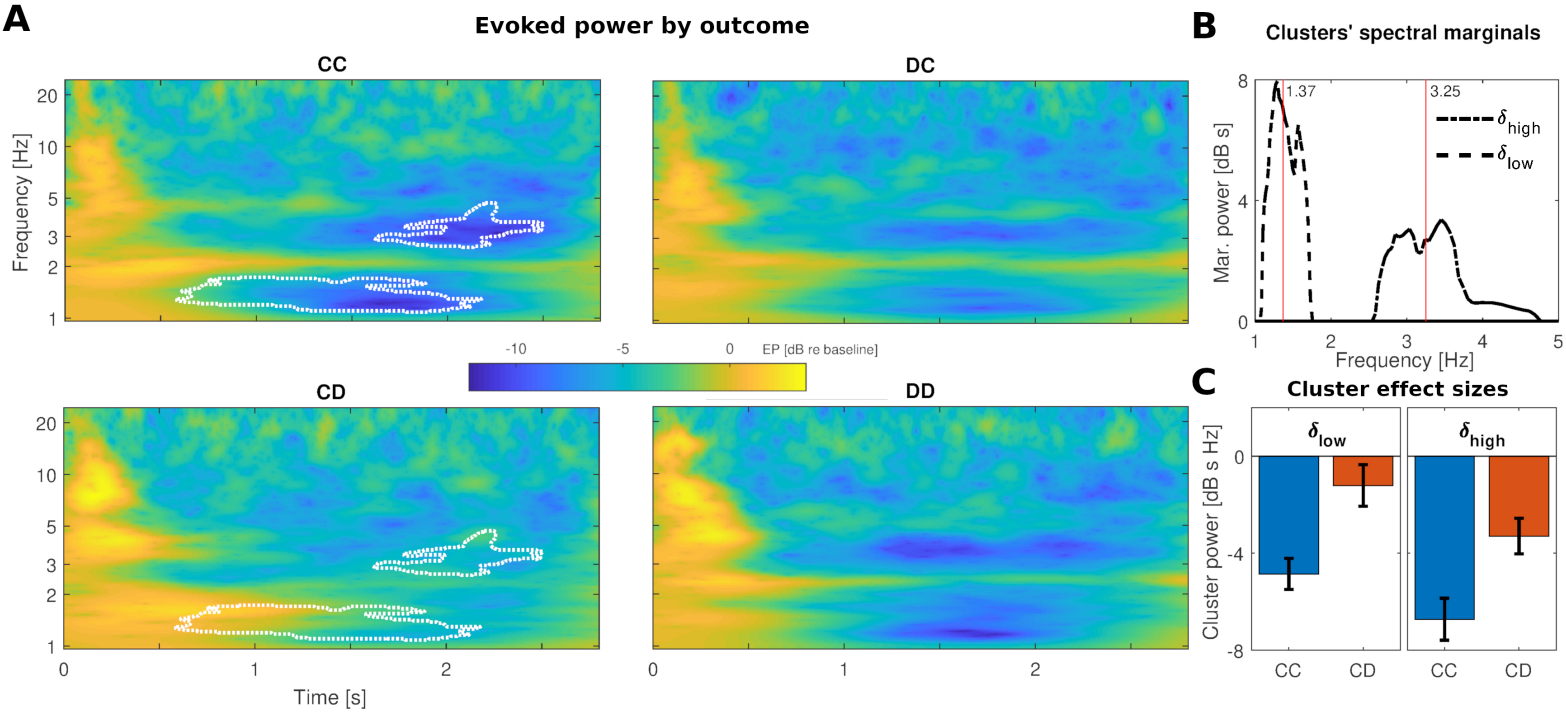

Figure 3. Time-frequency decomposition of LP data. (A) Spectrotemporal wavelet correlograms by outcome reveal slow-wave (<5 Hz, delta) differential activity in the 0.5 – 2.5 s interval post feedback onset. It consists of evoked power baseline de-synchronizations for every outcome, except one-sided cooperation (CD). Cluster analyses for CC-CD contrasts show significant differences in two time-frequency regions, slow (δ_{low}, 0.5-2 s) and fast (δ_{high}, 1.5-2.5 approx.) delta-band rhythmic activity (p=0.041). The cluster boundaries are superimposed. No clusters were found for DC-DD contrast. (B) Spectral profiles of differential cluster activity show how they are predominantly contained in the delta band. (C) Effect sizes, defined as participants' evoked power integrated over relevant cluster region boundaries, show significant effects of cooperation by the coplayer, indicating relatively higher desynchronization for mutual cooperation outcomes.

p=0.16; d=0.34) components. For spectrotemporal data, C|CC trials were found to contain greater

demodulations of slow wave activity relative to D|CC trials, in the high-delta spectrotemporal power

region determined earlier (Figure 4A). A significant cluster within this region determined by non-parametric testing (half-maximum 3.6-4.3 Hz, 1.87-2.23 s; p=0.034), was found to be significant in terms of average trial (total) power differences at the subject level (t(15)=2.78; p=0.014; d=0.70) (Figure 4B). In the low-delta region (determined earlier), the same analysis failed to reveal any significant spectrotemporal cluster difference.

Unreciprocated cooperation / sucker's payoff. CD trials were analyzed depending on whether they were followed by player cooperation ('C|CD') or not ('D|CD'). We found FRN signals to be on average of greater amplitude for C|CD (0.58 ± 1.78 a.u., mean ± SD) versus D|CD (-0.63 ± 1.79 a.u.), and the difference was significant at the subject level (t(17)=3.53; p=0.003; Cohen's d=0.83) (Figures 4A and 4B). In addition, there was limited evidence for the P3 to be of higher amplitude for C|CD than D|CD (t(17)=2.09; p=0.052; d=0.49), LP waveform activity (t(17)=1.88; p=0.078; d=0.44), nor LP-delta power which did not show significant cluster differences.

One-sided defection. For DC trials partitioned by *next choice*, contrasts were made between the player switching to cooperation at the next round (C|DC), versus repeated non-cooperation (D|DC). One-sample t tests showed significant mean waveform differences for the P3 (t(20)=2.39; p=0.027; Cohen's d=0.52), with greater amplitudes for C|DC (205 ± 86 μV; mean ± SD) than D|DC (178 ± 67 μV) (Figure 4A,B). Significant subject-level modulations by forthcoming choice were not found for the LP (Z=1.61; p=0.11; N=21).

Mutual defection. Separation of DD trials by *next choice* allowed comparison of feedback processing between cases where the player may choose to turn to cooperation at the next round ('C|DD'), versus repeat non-cooperation ('D|DD'). No significant differences were found between these conditions in

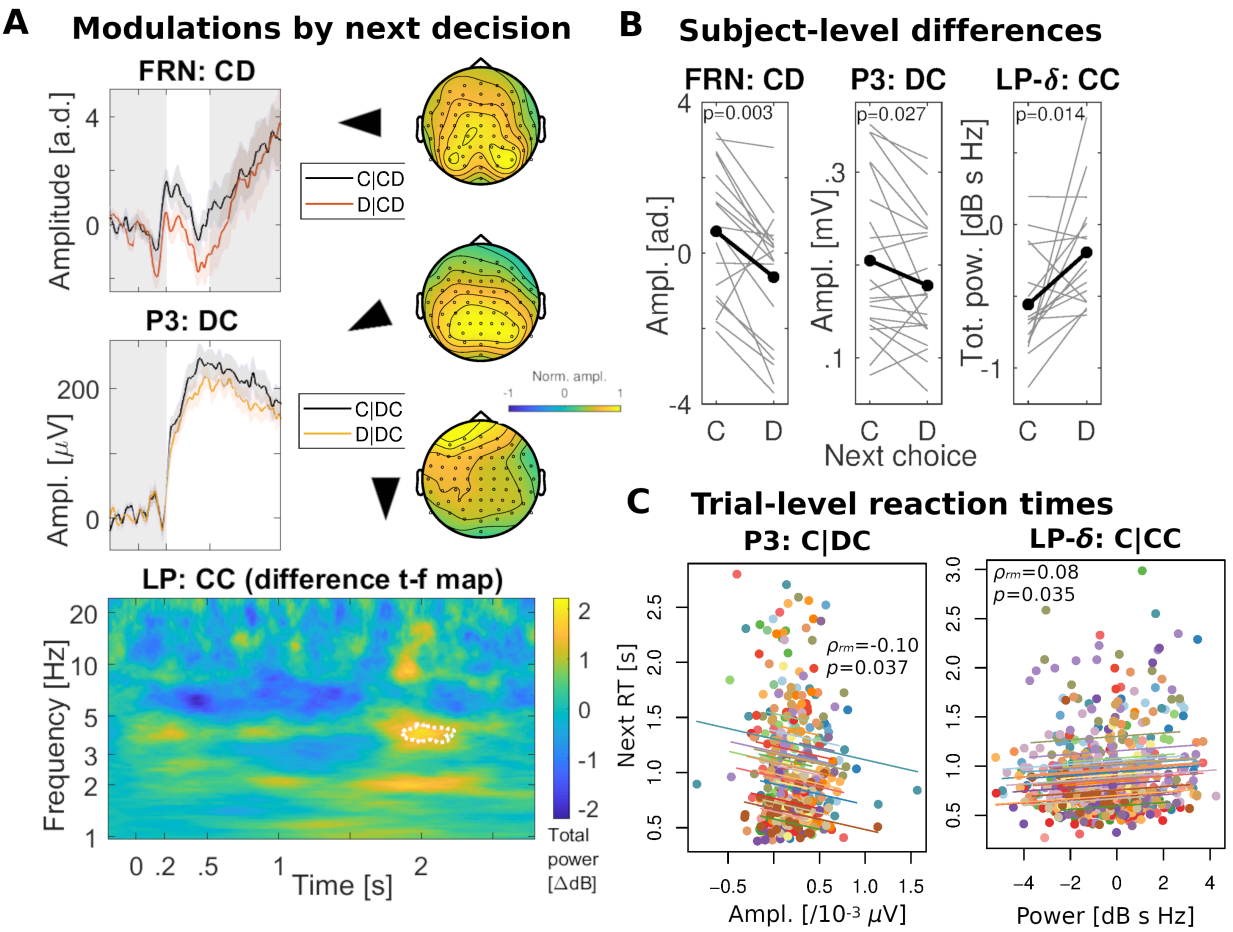

Figure 4. Next round decision-making at the iPD may be indicated by scalp activity related to current outcome processing, in a context-dependent manner. (A) Top: At unreciprocated cooperation outcomes (CD), centro-parietal ERP activity unfolds differentially according to the participant's decision at the subsequent round. Forthcoming non-cooperation may be accompanied by a lower-amplitude signal at this early stage of outcome-specific processing (0.2 – 0.5 s). Middle: For one-sided non-cooperation (DC), higher P3 amplitudes instead indicate forthcoming cooperation in average. Bottom: At mutual cooperation (CC), LP slow-wave activity is also differentially expressed, later, by subsequent round choice. The difference map in the total (trial) power correlogram (D|CC minus C|CC) is shown, with the significant difference cluster boundary superimposed. Topographies for each component are displayed. (B) Subject-level data of the three components and context in which they indicate next round decision-making, in grey. Grand average values are shown in black. (C) In the decision to maintain mutual cooperation further (C|CC), trial by trial variations in LP-delta power desynchronizations relate to the speed to which subjects respond at the next trial, with faster reaction times when LP-delta is more suppressed at the current trial.

the associated P3 ($t(22)=0.36$; $p=0.72$; Cohen's $d=0.08$), or LP ($t(22)=0.34$; $p=0.74$; $d=0.07$) waveforms.

To verify that *next choice* analyses were not a result of systematic bias explained by sample size imbalances across conditions, randomization tests were performed. Separately, and for each relevant outcome type and signal (namely, FRN from CD, P3 from DC, and LP-delta from CC), single trial data were randomly shuffled, across subsequent decisions to cooperate or not, per participant. This procedure created a spurious dataset where the original sample size imbalance was preserved, removing any empirical effect size. Randomization distributions of the effect sizes were generated by repeating the procedure multiple times (see Methods); the percentile of the empirical measure was computed as *p*-value. In this way, the previous C,D|CD FRN effect size was found to be significant with respect to the randomization distribution (p=0.018), as well as the C,D|DC P3 (p=0.026), and the C,D|CC LP-delta (p=0.002). These results indicated that *next choice* findings were not explained by potential systematic bias due to sample sizes.

Single trial reaction time analyses

Altogether, the results relate neural processing of iPD feedback to subsequent decision-making. By contrasting the temporal scales of effects on next-decision, it is suggested that CD and DC outcomes evoke earlier neural modulations indicative of participant behavior, while for the CC timecourse similar differential signaling begins considerably later. This signaling may each represent the temporal lower bounds of distinct decisional processes following each outcome context. Next-decision reaction time, on the other hand, indicates behavioral accomplishment and bounds the time dedicated to the decisional process from above. Behavioral reaction time data had indicated that CC outcomes may also elicit faster responses when participants are again prompted to make a choice at the next trial. This might suggest that CC cases may have effectively the shortest decision process (e.g. latest lower bound and earliest upper bound). Because the association between neural timecourse and behavioral reaction time

has an important source of variability in trial-by-trial decision-making, we investigated whether the FRN, P3 and LP-delta signals as found before may also indicate forthcoming reaction times. Repeated measures Pearson correlation coefficients[85] were computed to assess the relationship between signal trial amplitude for C,D|CD conditions, and subsequent reaction times. For FRN signals, no significant correlation was found for C|CD (ρ_{rm}(437)=-0.05, CI [-0.14, 0.04], p=0.31), nor for D|CD (ρ_{rm}(470)=-0.02, CI [-0.01, 0.06], p=0.66). For P3 signal trial amplitudes, the analysis revealed that in C|DC there is a significant negative correlation with subsequent trial reaction times (ρ_{rm}(422)=-0.101, CI [-0.196, -0.001], p=0.037). An increase in single trial P3 given DC outcomes was correlated with faster reaction times at the next trial involving participant cooperation (Figure 4C). There was no significant correlation under D|DC conditions however, ρ_{rm}(764)=-0.02, CI [-0.08, 0.04], p=0.62. Similarly, for LP-delta signals, a positive correlation between reaction time and LP-delta signals was found for C|CC conditions at the single trial level, ρ_{rm}(624)=0.084, CI [-0.001, 0.161], p=0.035. A reduction in LP-delta signals during CC feedback processing was correlated with faster reaction times at the next trial when cooperation was maintained (Figure 4C). By contrast, no correlation was found between LP-delta signals at D|CC trials and subsequent reaction time, ρ_{rm}(387)=-0.06, CI [-0.15, 0.04], p=0.26. The results suggest that processing of co-player's cooperation in the P3 or LP-delta (for DC or CC outcomes, respectively) may indicate how expedited will be reciprocative action at the subsequent trial.

Discussion

The findings confirm that, as part of feedback processing, ERP waveform components FRN and P3, but also a late, left-frontal LP and associated slow-wave delta-band activity (LP-delta) altogether encode aspects of *observed* cooperative choice at the iPD. Importantly, our results indicate that differential

processes *prospective* of subsequent cooperation may in addition be reflected in FRN, P3 and LP-delta components. This depends on the outcome scenario: (i) at unreciprocated cooperation (CD), where downmodulations to the FRN may indicate forthcoming non-cooperation; (ii) at one-sided defection (DC), where greater P3 amplitude is associated with a player's switch to cooperate next; and (iii) at mutual cooperation (CC), for which LP-delta power reductions relate to maintenance of cooperation at the next round. Finally, single trial P3 activation at DC rounds and, separately, LP-delta deactivation at CC rounds, entailed shortening of the time *to cooperate in reciprocity*. We propose that these modulations may be consistent with the deployment of 'automatic' or intuitive decision-making modes. We next discuss the role of each feedback component, and later relate them to the distinct social judgments involved in the decision to cooperate after each outcome type.

Electrophysiological responses to presented feedback

N1. The visual N1 sensory signal may arise from spatial generators in dorsal anterior occipital cortex, lateral extrastriate and posterior temporal regions[86], as well as the ventral extrastriate cortex of the fusiform gyrus[87]. It is susceptible to modulations of higher order perceptual processing[88], notably attention[89–91]. Importantly, our findings of increased N1 with cooperative choices during feedback processing were only indicated by a non-significant trend. This effect would be consistent with the attentional interpretation of greater evoked N1 activity, which might be due to the participant's higher stakes in terms of expected return (e.g. by emotional scores), in cases where she/he has already chosen to cooperate.

FRN. The FRN is a widely analyzed component in reward processing studies, and it is considered to be related to the evaluation of reward outcome conditions[25,33,36]. Its source has been consistently reported at

the anterior cingulate cortex (ACC)[30,33,92], in some cases with contributions from posterior cingulate cortex (PCC)[33,66,93,94] and the basal ganglia[95]. We provide a data-driven means to extract it, by addressing the separation between (long-term optimal) CC and (emotionally worst) CD outcomes. While our results appear more posterior than topographies associated with the ACC, they are consistent with a centroparietal distribution, which was found related to a PCC source, in a previous FRN study[36]. The PCC is functionally heterogeneous and reflects preferential activation for positive reward[93], as well as high sensitivity to arousal state[96]. Its ventral subdivision is involved in emotional events and default mode network[96,97], while the dorsal part is active during theory of mind tasks[30] and shows connectivity to frontal regions for cognitive control and behavioral change[96,98]. Both subdivisions are relevant for prospective decision-making in social exchange tasks.

Both Gheza and colleagues[36] and our study introduce data-driven methods based on grand average information from the 0.2-0.5 s window, where the FRN is typically found[31,32]. This spatial profile was interpreted in the Gheza et al. study as a *reward positivity*[36] (but see e.g.[99] for a review of this component), since a distinct profile was observed transiently for non-rewarded conditions, which they termed *feedback-related negativity.* The Gheza et al. *reward positivity* component, which closely resembles our FRN, was the most consistent activity profile across reward conditions in their study for the same interval as ours. It is therefore possible that our estimation method, based on a difference waveform bias[35], successfully captured the relative imbalance between both spatial profiles (i.e., *reward positivity* and *feedback-related negativity* as in[36]) into a single component reflecting the effective distance between rewarded (CC) versus non-rewarded (CD) spatial activity profiles over time. Here, we refer to such (combined) component as FRN.

The suggestion that discrimination between reward presence and absence may be effected by transient pausing of dopaminergic firing during no-reward outcomes[36], is consistent with computation of reward prediction error[31,100], or of unsigned feedback saliency[34,101,102]. Animal data have shown that cingulate

activity modulations, associated to the FRN, also persist at the subsequent decision-making stage and even predict behavior[103,104]. Such activity may serve to adapt decision-related behavior by updating and integrating feedback history over time[105,106], which can be harnessed to predict a participant strategy change during economic games[66]. We may interpret 'pausing' of FRN activity after CD outcomes (relative to CC) in this framework, which takes place further if preceding non-cooperation at the next round. A participant's choice to cooperate leading to 'sucker's payoff' may be based on erroneous estimation that the co-player would also cooperate, thus, the outcome may represent an update towards her/his original expectation, by signaling via FRN downmodulations. When such downmodulations are particularly strong, the participant may be unlikely to cooperate next. It remains unclear if the hypothesized 'pausing', as measured in the FRN, might provide indication of the previously held expectation by the player about the co-player's action, and/or the intrinsic value that a CC event would have had for the player. The first alternative may require internal models about the co-player (e.g., trust valuations), integrating predictive computations from social processing systems. The second may be potentially based on learning from evidence over time, as well as on emotional heuristics as proxy for prediction[30,107,108].

P3. P3 sources have been associated to the temporo-parietal junction (TPJ)[109], with contributions from noradrenergic arousal systems[39,48]. The TPJ underpins processing of affective and emotional attributes[110–116], social interactions, peer comparisons, trust/familiarity, and group outcomes[79,117,118,24,119]. P3 activation in social dilemmas includes the chicken game[120,121], prisoner's dilemma[26,27], dictator[122], and ultimatum games[123–127]. Our data shows that the P3 is modulated by the co-player's choice to cooperate, consistent with increased P3 levels for positive reward. The player's choice to cooperate, which by itself does not guarantee a positive reward, also effects a modulation over the P3. This is consistent with the P3 role in engagement by the attentional and arousal systems, given the player's

relatively higher stakes in risking to cooperate but also the involvement of memory and learning systems regarding further action[44]. CC outcomes appeared to yield greater P3 modulations, which may be consistent with a "temporal filtering"[128,129] model of noradrenergic function considering the relative adaptive value of mutual cooperation events for the task. The modulations may indicate specific engagement of attentional and memory encoding systems for these outcomes because they directly increase the likelihood for sustained mutual cooperation in the long run.

LP. In terms of latency, the LP observed in our data is consistent with the late positive potential ('LPP'), a feedback component related to emotional processing. However, on a spatial basis, the LPP typically follows a posterior scalp distribution associated with visual cortical areas[25,116] (see[130] for a more frontal distribution). The LPP also displays a positive bias for negative stimuli or losses in emotion as well as in value-based decision making studies[25,116,130,131], whereas the observed LP showed more positive values for positive outcomes instead. In order to interpret this component, it may be important to consider its frontal asymmetry[132]. Memory and emotional processes may be involved in frontal EEG asymmetries: first, the *hemispheric encoding and retrieval asymmetry model* posits that episodic memory encoding is more dominantly undertaken by the left prefrontal cortex (PFC), while right PFC may be involved in episodic memory retrieval[133,134]. The 0.5-0.9 s interval can be critical for memory retrieval[135], a process that can be substantially impaired by stimulation to left dorsolateral PFC and neighboring regions over the same temporal window[136,137]. Therefore, the earlier part of the observed LP could involve interactions between memory and context updating processes reflected at the later stage of the P3. This may be consistent with frontoparietal network models of working memory[138]. Second, frontal EEG asymmetries are addressed in the *approach-withdrawal motivational model*[139–142], which proposes that left frontal activity supports approach motivation induced by emotional stimuli[143,144] and reward[145,146], whereas it inhibits negative or withdrawal-related

information[10,147]. Left bias measures are typically expressed in terms of alpha-band oscillatory power[148], particularly of dorsolateral PFC[149] sources, and such band activity has been considered to negatively correlate with cortical processing[150,151]. In agreement with the approach motivation interpretation, there are reports of left prefrontal EEG modulation in cooperative interpersonal tasks relating self-perception of social ranking[152] or power[153,154] for instance. Thus, it appears our findings might also be consistent with the interpretation that co-player cooperation may induce an approach-oriented state towards the partner.

LP-delta. Based on spectrotemporal decomposition of the LP scalp topography waveform (e.g.[155]), the results show a suppression of slow-wave LP-delta activity for mutual versus unreciprocated cooperation. Frontal regions are not the only cortical sources for delta activity, but may include medial and ventral frontal cortex[156–159]; moreover, the delta rhythm can be modulated by left dorsolateral PFC stimulation[160]. Delta-band activity has been proposed to integrate homeostatic information with cortical processes in reward and emotional systems[161,162], where reductions may indicate more positive and/or less anxiogenic (more relaxed) states[163]. Delta-band upmodulations, on the other hand, have been involved in increased attention states (e.g., by arousing pictures and emotional faces[155,162,164]), and heightened concentration[165] at tasks requiring control over inhibitory capabilities[166]. Our results may then provide support for the interpretation of a “relief” neural signal following mutual cooperation, which does not take place after ‘sucker’s payoff’ outcomes. In addition, frontal delta increases in the literature have been suggested to modulate other activity distal from the frontal lobes, including sensory afferences that may interfere with the task at hand[165]. Downmodulations of frontal delta-band activity may as well indicate differential processing of positive relative to negative probabilistic alternatives[167] and feedback[168]. While in general prefrontal areas signal upcoming decisions during outcome evaluation[169], left hemisphere activity has been associated to specializations for planning,

control, and predictive model updating[170,171]. The processes supported across these networks include the learning and representation of option values[172–175], socio-emotional perspective taking[176,177], and the combining of choice-based with value-based sources of information[178]. Its suppression would appear consistent with the inhibition of mechanisms that alter homeostasis, as a consequence of having prevented the worst outcome. As discussed below, this inhibitory mechanism might provide a basis for promoting cooperation in a more 'automatic' manner.

Outcome context-dependence and decision-making at the iterated PD

Our data showed that neural activity at the feedback stage may not only reflect representations of players' choices leading to the current outcome. It also entails early indices of processes underlying decision-making at the subsequent round. The type of outcome critically affects which of these processes intervene, and when. For instance, 'sucker's payoff' represents a worst-case outcome, interpretable as a cooperation error. Our results of FRN downregulation within an early window (0.2 to 0.5 s) for CD trials suggest the FRN operates effectively as a detection system for round failure at the iPD. Because choosing not to cooperate after CD was associated to relatively more FRN downregulation, the results also suggest a heuristic for subsequent decision in this context. The encoded violation of expected reciprocity or salience may assist in adjusting representations about choice alternatives[66]. Further studies may address whether the FRN role is better described in terms of saliency of effected non-cooperative choice by the co-player, or prior expectation about her/his likelihood to cooperate[33].

After mutual cooperation events, LP-delta deactivations were found to be modulated depending on whether the participant would sustain cooperation further. This differential process was observed at

greater latency (~2 s) than analogous FRN (at CD) and P3 (at DC, 0.2 to 1 s) effects. This does not imply more 'deliberative' decision-making after CC, however. It suggests that the aftermath of mutual cooperation may entail a subsequent decisional process with relatively longer latency to begin. We nevertheless verified that such LP-delta deactivations also preceded reduced reaction times – provided that, at the next trial, cooperation was exerted by the player. We suggest that both findings in effect constrain the timecourse of the decision process. As discussed earlier, delta activity changes may be related to self-adjusting mechanisms of homeostasis. If instantiated at frontal networks, where judgment and selection systems guide further action, we conjecture such modulations may effectively represent a value signal[168], or an anticipatory or belief state (e.g. [27]). Future studies may address directly the interpretation of frontal delta baseline activity, and clarify whether its deactivations represent value signals or updating processes[179].

A similar dual finding was observed for P3 activations following DC trials. P3 was increased on average when the next decision was to cooperate than when it was not; it also increased on a trial basis preceding decisions to cooperate taken more quickly. The results may be interpreted in terms of player-based surprise or saliency about DC events, if he/she did not expect cooperation from the co-player. We propose that after DC, decisions may primarily rely on estimating co-player likelihood of reciprocating defection or seeking cooperation. For this, a heuristic of conflict violation or saliency estimation may need to be framed from the co-player perspective, based on group-level outcomes and partner comparisons. Such a 'reflector' prediction model may in principle require contributions from theory of mind, working memory and planning systems, which may be subserved across parietal networks[180–182].

Together with LP-delta findings, the results indicate that the specific case of 'C|XC' trials (that is, where the player cooperates subsequent to the co-player) lead to more "automatic" modes of

cooperation, predictable from relevant EEG scalp activity at the last feedback update. It is worth noting that behavioral analyses had indicated that reaction times preceded by CC outcomes were on average shorter than when preceded by DC, and that LP-delta effects were observed ~1 s later than P3. These results point to the action to cooperate after mutual cooperation as involving a shorter decisional process, underpinned by neural modulation interpretable in homeostatic terms. Because of the relatively earlier timing of P3, future studies on cooperative heuristics may further address aspects of conscious access[183] to the processes involved in updating internal models about a partner. We suggest these findings relate to analyses of decision-making heuristics that reduce deliberation, as an important context shaping such heuristics[69,70,184].

Conclusion

Comprehensive descriptions of feedback signals involved in the iterated prisoner's dilemma may serve to identify which of them relate to subsequent cooperation and how. Due to the economic structure of the game, each outcome affects the type of strategic predictions that are relevant for a player to make for the next round, given the present cooperation context. The findings demonstrate that the capacity for feedback signals to relate future cooperation falls along the same contingencies; in effect, such signals also 'tag' in time the moment at which evidence integration may begin to index next decision-making. For the specific action of *reciprocating mutual cooperation*, expedited executions were associated to the same feedback processes. The results support the existence of cognitive systems for fast decision-making[68,185], including on whether to cooperate in social dilemmas[69–71], in part related to predictive coding – an efficiency-based account of cortical function[179,186,187]. We suggest there is an association between both frameworks in the use of social heuristics, in cases where quick and intuitive appraisals may improve the returns over more sustained and deliberate prospect-making.

Competing interests statement

Declarations of interest: none

Acknowledgements

This study was funded by *Proyectos I+D* from the Comisión Sectorial de Investigación Científica, Universidad de la República (UdelaR, Uruguay), and by *Fondo Santiago Achúgar Díaz* 2018 from the Programa de Desarrollo de las Ciencias Básicas (PEDECIBA, Uruguay). We thank support to FCC by the *Becas de Posdoctorado* from the Agencia Nacional de Investigación e Innovación (ANII, Uruguay). We thank funding support to DK from grants *Ayudas a la Atracción de Talento Investigador* (2017-T2/SOC-5569) from the Comunidad de Madrid and the Universidad Autónoma de Madrid (Spain), and *PGC2018-093570-B-I00* from the Ministerio de Ciencia, Innovación y Universidades (Spain). We also thank funding support to AC and VBG from UdelaR and ANII. None of the funding sources had a role in study design, data collection, analysis or interpretation of data, nor writing or submission of the report for publication.

References

1. Axelrod, R. & Hamilton, W. D. The evolution of cooperation. *Science* **211**, 1390–1396 (1981).
2. Flood, M. M. Some Experimental Games. *Manag. Sci.* **5**, 5–26 (1958).
3. Rapoport, A. & Chammah, A. M. *Prisoner's dilemma: a study in conflict and cooperation*. (University of Michigan Press, 1965).
4. Rilling, J. K. *et al.* A Neural Basis for Social Cooperation. *Neuron* **35**, 395–405 (2002).
5. Rilling, J. K., Sanfey, A. G., Aronson, J. A., Nystrom, L. E. & Cohen, J. D. The neural correlates of theory of mind within interpersonal interactions. *NeuroImage* **22**, 1694–1703 (2004).
6. Singer, T., Kiebel, S. J., Winston, J. S., Dolan, R. J. & Frith, C. D. Brain responses to the acquired moral status of faces. *Neuron* **41**, 653–662 (2004).
7. Rilling, J. K. *et al.* The neural correlates of the affective response to unreciprocated cooperation. *Neuropsychologia* **46**, 1256–1266 (2008).
8. Krach, S. *et al.* Are women better mindreaders? Sex differences in neural correlates of mentalizing detected with functional MRI. *BMC Neurosci.* **10**, 9 (2009).

9. Kircher, T. *et al.* Online mentalising investigated with functional MRI. *Neurosci. Lett.* **454**, 176–181 (2009).

10. Suzuki, S., Niki, K., Fujisaki, S. & Akiyama, E. Neural basis of conditional cooperation. *Soc. Cogn. Affect. Neurosci.* **6**, 338–347 (2011).

11. Ramsøy, T. Z., Skov, M., Macoveanu, J., Siebner, H. R. & Fosgaard, T. R. Empathy as a neuropsychological heuristic in social decision-making. *Soc. Neurosci.* **10**, 179–191 (2015).

12. Etzel, J. A., Valchev, N., Gazzola, V. & Keysers, C. Is Brain Activity during Action Observation Modulated by the Perceived Fairness of the Actor? *Plos One* **11**, e0145350 (2016).

13. Lambert, B., Declerck, C. H., Emonds, G. & Boone, C. Trust as commodity: social value orientation affects the neural substrates of learning to cooperate. *Soc. Cogn. Affect. Neurosci.* **12**, 609–617 (2017).

14. Rilling, J. K. *et al.* Neural correlates of social cooperation and non-cooperation as a function of psychopathy. *Biol. Psychiatry* **61**, 1260–1271 (2007).

15. McClure-Tone, E. B. *et al.* Preliminary Findings: Neural Responses to Feedback Regarding Betrayal and Cooperation in Adolescent Anxiety Disorders. *Dev. Neuropsychol.* **36**, 453–472 (2011).

16. Rilling, J. K. *et al.* Sex differences in the neural and behavioral response to intranasal oxytocin and vasopressin during human social interaction. *Psychoneuroendocrinology* **39**, 237–248 (2014).

17. Schneider-Hassloff, H., Straube, B., Nuscheler, B., Wemken, G. & Kircher, T. Adult attachment style modulates neural responses in a mentalizing task. *Neuroscience* **303**, 462–473 (2015).

18. Feng, C. *et al.* Oxytocin and vasopressin effects on the neural response to social cooperation are modulated by sex in humans. *Brain Imaging Behav.* **9**, 754–764 (2015).

19. Chen, X. *et al.* Effects of oxytocin and vasopressin on the neural response to unreciprocated cooperation within brain regions involved in stress and anxiety in men and women. *Brain Imaging Behav.* **10**, 581–593 (2016).

20. Zheng, H., Kendrick, K. M. & Yu, R. Fear or greed? Oxytocin regulates inter-individual conflict by enhancing fear in men. *Horm. Behav.* **85**, 12–18 (2016).

21. Gradin, V. B. *et al.* Neural correlates of social exchanges during the Prisoner's Dilemma game in depression. *Psychol. Med.* **46**, 1289–1300 (2016).

22. Fallani, F. D. V. *et al.* Defecting or Not Defecting: How to 'Read'' Human Behavior during Cooperative Games by EEG Measurements'. *Plos One* **5**, e14187 (2010).

23. Jahng, J., Kralik, J. D., Hwang, D.-U. & Jeong, J. Neural dynamics of two players when using nonverbal cues to gauge intentions to cooperate during the Prisoner's Dilemma Game. *Neuroimage* **157**, 263–274 (2017).

24. Hu, Y. *et al.* Inter-brain synchrony and cooperation context in interactive decision making. *Biol. Psychol.* **133**, 54–62 (2018).

25. Glazer, J. E., Kelley, N. J., Pornpattananangkul, N., Mittal, V. A. & Nusslock, R. Beyond the FRN: Broadening the time-course of EEG and ERP components implicated in reward processing. *Int. J. Psychophysiol.* **132**, 184–202 (2018).

26. Bell, R. *et al.* Event-related potentials in response to cheating and cooperation in a social dilemma game. *Psychophysiology* **53**, 216–228 (2016).

27. Zhang, D., Lin, Y., Jing, Y., Feng, C. & Gu, R. The Dynamics of Belief Updating in Human Cooperation: Findings from inter-brain ERP hyperscanning. *NeuroImage* **198**, 1–12 (2019).

28. Ravaja, N., Bente, G., Katsyri, J., Salminen, M. & Takala, T. Virtual Character Facial Expressions Influence Human Brain and Facial EMG Activity in a Decision-Making Game. *Ieee Trans. Affect. Comput.* **9**, 285–298 (2018).

29. Picton, T. W. *Human auditory evoked potentials*. (Plural Pub, 2010).

30. Walsh, M. M. & Anderson, J. R. Learning from experience: event-related potential correlates of reward processing, neural adaptation, and behavioral choice. *Neurosci. Biobehav. Rev.* **36**, 1870–1884 (2012).

31. Sambrook, T. D. & Goslin, J. A neural reward prediction error revealed by a meta-analysis of ERPs using great grand averages. *Psychol. Bull.* **141**, 213–235 (2015).

32. Ullsperger, M., Fischer, A. G., Nigbur, R. & Endrass, T. Neural mechanisms and temporal dynamics of performance monitoring. *Trends Cogn. Sci.* **18**, 259–267 (2014).

33. Hauser, T. U. *et al.* The feedback-related negativity (FRN) revisited: new insights into the localization, meaning and network organization. *NeuroImage* **84**, 159–168 (2014).

34. Talmi, D., Atkinson, R. & El-Deredy, W. The feedback-related negativity signals salience prediction errors, not reward prediction errors. *J. Neurosci. Off. J. Soc. Neurosci.* **33**, 8264–8269 (2013).

35. de Cheveigné, A. & Parra, L. C. Joint decorrelation, a versatile tool for multichannel data analysis. *NeuroImage* **98**, 487–505 (2014).

36. Gheza, D., Paul, K. & Pourtois, G. Dissociable effects of reward and expectancy during evaluative feedback processing revealed by topographic ERP mapping analysis. *Int. J. Psychophysiol. Off. J. Int. Organ. Psychophysiol.* **132**, 213–225 (2018).

37. Sutton, S., Braren, M., Zubin, J. & John, E. R. Evoked-potential correlates of stimulus uncertainty. *Science* **150**, 1187–1188 (1965).

38. Kok, A. On the utility of P3 amplitude as a measure of processing capacity. *Psychophysiology* **38**, 557–577 (2001).

39. Nieuwenhuis, S., Aston-Jones, G. & Cohen, J. D. Decision making, the P3, and the locus coeruleus-norepinephrine system. *Psychol. Bull.* **131**, 510–532 (2005).

40. Duncan, C. C. *et al.* Event-related potentials in clinical research: guidelines for eliciting, recording, and quantifying mismatch negativity, P300, and N400. *Clin. Neurophysiol. Off. J. Int. Fed. Clin. Neurophysiol.* **120**, 1883–1908 (2009).

41. Polich, J. Neuropsychology of P300. in *The Oxford handbook of event-related potential components* 159–188 (Oxford University Press, 2012).

42. Luck, S. J. *An Introduction to the Event-Related Potential Technique*. (MIT Press, 2014).

43. Donchin, E. & Coles, M. G. Is the P300 component a manifestation of context updating? *Behav. Brain Sci.* **11**, 357–427 (1988).

44. Polich, J. Updating P300: an integrative theory of P3a and P3b. *Clin. Neurophysiol. Off. J. Int. Fed. Clin. Neurophysiol.* **118**, 2128–2148 (2007).

45. Feldman, H. & Friston, K. Attention, Uncertainty, and Free-Energy. *Front. Hum. Neurosci.* **4**, (2010).

46. Twomey, D. M., Murphy, P. R., Kelly, S. P. & O'Connell, R. G. The classic P300 encodes a build-to-threshold decision variable. *Eur. J. Neurosci.* **42**, 1636–1643 (2015).

47. McCarthy, G. & Donchin, E. A metric for thought: a comparison of P300 latency and reaction time. *Science* **211**, 77–80 (1981).

48. Warren, C. M., Nieuwenhuis, S. & Donner, T. H. Perceptual choice boosts network stability: effect of neuromodulation? *Trends Cogn. Sci.* **19**, 362–364 (2015).

49. San Martín, R. Event-related potential studies of outcome processing and feedback-guided learning. *Front. Hum. Neurosci.* **6**, 304 (2012).

50. Yeung, N. & Sanfey, A. G. Independent coding of reward magnitude and valence in the human brain. *J. Neurosci. Off. J. Soc. Neurosci.* **24**, 6258–6264 (2004).

51. Hajcak, G., Holroyd, C. B., Moser, J. S. & Simons, R. F. Brain potentials associated with expected and unexpected good and bad outcomes. *Psychophysiology* **42**, 161–170 (2005).

52. Sato, A. *et al.* Effects of value and reward magnitude on feedback negativity and P300. *Neuroreport* **16**, 407–411 (2005).

53. Wu, Y. & Zhou, X. The P300 and reward valence, magnitude, and expectancy in outcome evaluation. *Brain Res.* **1286**, 114–122 (2009).

54. Zhou, Z., Yu, R. & Zhou, X. To do or not to do? Action enlarges the FRN and P300 effects in outcome evaluation. *Neuropsychologia* **48**, 3606–3613 (2010).

55. Polezzi, D., Sartori, G., Rumiati, R., Vidotto, G. & Daum, I. Brain correlates of risky decision-making. *NeuroImage* **49**, 1886–1894 (2010).

56. Wang, L., Zheng, J., Huang, S. & Sun, H. P300 and Decision Making Under Risk and Ambiguity. *Intell Neurosci.* **2015**, 1:1–1:1 (2015).

57. Mei, S., Li, Q., Liu, X. & Zheng, Y. Monetary Incentives Modulate Feedback-related Brain Activity. *Sci. Rep.* **8**, 11913 (2018).

58. Severo, M. C., Walentowska, W., Moors, A. & Pourtois, G. Goals matter: Amplification of the motivational significance of the feedback when goal impact is increased. *Brain Cogn.* **128**, 56–72 (2018).

59. Fischer, A. G. & Ullsperger, M. Real and Fictive Outcomes Are Processed Differently but Converge on a Common Adaptive Mechanism. *Neuron* **79**, 1243–1255 (2013).

60. Chase, H. W., Swainson, R., Durham, L., Benham, L. & Cools, R. Feedback-related Negativity Codes Prediction Error but Not Behavioral Adjustment during Probabilistic Reversal Learning. *J. Cogn. Neurosci.* **23**, 936–946 (2010).

61. San Martín, R., Appelbaum, L. G., Pearson, J. M., Huettel, S. A. & Woldorff, M. G. Rapid brain responses independently predict gain-maximization and loss-minimization during economic decision-making. *J. Neurosci. Off. J. Soc. Neurosci.* **33**, 7011–7019 (2013).

62. Zhang, D. *et al.* Linking brain electrical signals elicited by current outcomes with future risk decision-making. *Front. Behav. Neurosci.* **8**, (2014).

63. Eppinger, B., Walter, M. & Li, S.-C. Electrophysiological correlates reflect the integration of model-based and model-free decision information. *Cogn. Affect. Behav. Neurosci.* **17**, 406–421 (2017).

64. Pisauro, M. A., Fouragnan, E., Retzler, C. & Philiastides, M. G. Neural correlates of evidence accumulation during value-based decisions revealed via simultaneous EEG-fMRI. *Nat. Commun.* **8**, 15808 (2017).

65. Wichary, S., Magnuski, M., Oleksy, T. & Brzezicka, A. Neural Signatures of Rational and Heuristic Choice Strategies: A Single Trial ERP Analysis. *Front. Hum. Neurosci.* **11**, (2017).

66. Cohen, M. X. & Ranganath, C. Reinforcement learning signals predict future decisions. *J. Neurosci. Off. J. Soc. Neurosci.* **27**, 371–378 (2007).

67. Kahneman, D. A perspective on judgment and choice: mapping bounded rationality. *Am. Psychol.* **58**, 697–720 (2003).

68. Kahneman, D. *Thinking, Fast and Slow*. (Penguin Books, 2012).

69. Bear, A. & Rand, D. G. Intuition, deliberation, and the evolution of cooperation. *Proc. Natl. Acad. Sci.* **113**, 936–941 (2016).

70. Rand, D. G. Cooperation, Fast and Slow: Meta-Analytic Evidence for a Theory of Social Heuristics and Self-Interested Deliberation. *Psychol. Sci.* **27**, 1192–1206 (2016).

71. Jagau, S. & van Veelen, M. A general evolutionary framework for the role of intuition and deliberation in cooperation. *Nat. Hum. Behav.* **1**, 0152 (2017).

72. Peirce, J. W. PsychoPy—Psychophysics software in Python. *J. Neurosci. Methods* **162**, 8–13 (2007).

73. Kalma, A. P., Visser, L. & Peeters, A. Sociable and aggressive dominance: Personality differences in leadership style? *Leadersh. Q.* **4**, 45–64 (1993).

74. Cook, J. L., den Ouden, H. E. M., Heyes, C. M. & Cools, R. The Social Dominance Paradox. *Curr. Biol.* **24**, 2812–2816 (2014).

75. Buunk, A. P. & Fisher, M. Individual differences in intrasexual competition. *J. Evol. Psychol.* **7**, 37–48 (2009).

76. Junghöfer, M., Elbert, T., Tucker, D. M. & Rockstroh, B. Statistical control of artifacts in dense array EEG/MEG studies. *Psychophysiology* **37**, 523–532 (2000).

77. Cohen, M. X. Comparison of linear spatial filters for identifying oscillatory activity in multichannel data. *J. Neurosci. Methods* **278**, 1–12 (2017).

78. de Cheveigné, A. & Simon, J. Z. Denoising based on spatial filtering. *J. Neurosci. Methods* **171**, 331–339 (2008).

79. Boksem, M. A. S., Kostermans, E. & De Cremer, D. Failing where others have succeeded: Medial Frontal Negativity tracks failure in a social context. *Psychophysiology* **48**, 973–979 (2011).

80. Makeig, S. Auditory event-related dynamics of the EEG spectrum and effects of exposure to tones. *Electroencephalogr. Clin. Neurophysiol.* **86**, 283–293 (1993).

81. Makeig, S., Debener, S., Onton, J. & Delorme, A. Mining event-related brain dynamics. *Trends Cogn. Sci.* **8**, 204–210 (2004).

82. Maris, E. & Oostenveld, R. Nonparametric statistical testing of EEG- and MEG-data. *J. Neurosci. Methods* **164**, 177–190 (2007).

83. Maris, E. Statistical testing in electrophysiological studies. *Psychophysiology* **49**, 549–565 (2012).

84. Edgington, E. & Onghena, P. *Randomization Tests*. (Chapman & Hall/CRC, 2007).

85. Bakdash, J. Z. & Marusich, L. R. Repeated Measures Correlation. *Front. Psychol.* **8**, (2017).

86. Clark, V. P., Fan, S. & Hillyard, S. A. Identification of early visual evoked potential generators by retinotopic and topographic analyses. *Hum. Brain Mapp.* **2**, 170–187 (1994).

87. Russo, F. D., Martínez, A., Sereno, M. I., Pitzalis, S. & Hillyard, S. A. Cortical sources of the early components of the visual evoked potential. *Hum. Brain Mapp.* **15**, 95–111 (2002).

88. Ahmadi, M., McDevitt, E. A., Silver, M. A. & Mednick, S. C. Perceptual learning induces changes in early and late visual evoked potentials. *Vision Res.* **152**, 101–109 (2018).

89. Luck, S. J., Fan, S. & Hillyard, S. A. Attention-related modulation of sensory-evoked brain activity in a visual search task. *J. Cogn. Neurosci.* **5**, 188–195 (1993).

90. Noesselt, T. *et al.* Delayed striate cortical activation during spatial attention. *Neuron* **35**, 575–587 (2002).

91. Martinez, A., Ramanathan, D. S., Foxe, J. J., Javitt, D. C. & Hillyard, S. A. The role of spatial attention in the selection of real and illusory objects. *J. Neurosci. Off. J. Soc. Neurosci.* **27**, 7963–7973 (2007).

92. Gehring, W. J. & Willoughby, A. R. The medial frontal cortex and the rapid processing of monetary gains and losses. *Science* **295**, 2279–2282 (2002).

93. Liu, X., Hairston, J., Schrier, M. & Fan, J. Common and distinct networks underlying reward valence and processing stages: a meta-analysis of functional neuroimaging studies. *Neurosci. Biobehav. Rev.* **35**, 1219–1236 (2011).

94. Nieuwenhuis, S., Slagter, H. A., von Geusau, N. J. A., Heslenfeld, D. J. & Holroyd, C. B. Knowing good from bad: differential activation of human cortical areas by positive and negative outcomes. *Eur. J. Neurosci.* **21**, 3161–3168 (2005).

95. Foti, D., Weinberg, A., Bernat, E. M. & Proudfit, G. H. Anterior cingulate activity to monetary loss and basal ganglia activity to monetary gain uniquely contribute to the feedback negativity. *Clin. Neurophysiol. Off. J. Int. Fed. Clin. Neurophysiol.* **126**, 1338–1347 (2015).

96. Leech, R. & Sharp, D. J. The role of the posterior cingulate cortex in cognition and disease. *Brain* **137**, 12–32 (2014).

97. Vogt, B. A. Pain and Emotion Interactions in Subregions of the Cingulate Gyrus. *Nat. Rev. Neurosci.* **6**, 533–544 (2005).

98. Bzdok, D. *et al.* Subspecialization in the human posterior medial cortex. *NeuroImage* **106**, 55–71 (2015).

99. Proudfit, G. H. The reward positivity: from basic research on reward to a biomarker for depression. *Psychophysiology* **52**, 449–459 (2015).

100. Warren, C. M. & Holroyd, C. B. The Impact of Deliberative Strategy Dissociates ERP Components Related to Conflict Processing vs. Reinforcement Learning. *Front. Neurosci.* **6**, 43 (2012).

101. Heydari, S. & Holroyd, C. B. Reward positivity: Reward prediction error or salience prediction error? *Psychophysiology* **53**, 1185–1192 (2016).

102. Hird, E. J., El-Deredy, W., Jones, A. & Talmi, D. Temporal dissociation of salience and prediction error responses to appetitive and aversive taste. *Psychophysiology* **55**, e12976 (2018).

103. Fouragnan, E., Retzler, C., Mullinger, K. & Philiastides, M. G. Two spatiotemporally distinct value systems shape reward-based learning in the human brain. *Nat. Commun.* **6**, (2015).

104. Hayden, B. Y., Nair, A. C., McCoy, A. N. & Platt, M. L. Posterior cingulate cortex mediates outcome-contingent allocation of behavior. *Neuron* **60**, 19–25 (2008).

105. Hayden, B. Y., Nair, A. C., McCoy, A. N. & Platt, M. L. Posterior cingulate cortex mediates outcome-contingent allocation of behavior. *Neuron* **60**, 19–25 (2008).

106. Pearson, J. M., Heilbronner, S. R., Barack, D. L., Hayden, B. Y. & Platt, M. L. Posterior cingulate cortex: adapting behavior to a changing world. *Trends Cogn. Sci.* **15**, 143–151 (2011).

107. Houser, D. & McCabe, K. Chapter 2 - Experimental Economics and Experimental Game Theory. in *Neuroeconomics (Second Edition)* (eds. Glimcher, P. W. & Fehr, E.) 19–34 (Academic Press, 2014). doi:10.1016/B978-0-12-416008-8.00002-4

108. Li, D., Meng, L. & Ma, Q. Who Deserves My Trust? Cue-Elicited Feedback Negativity Tracks Reputation Learning in Repeated Social Interactions. *Front. Hum. Neurosci.* **11**, (2017).

109. Soltani, M. & Knight, R. T. Neural origins of the P300. *Crit. Rev. Neurobiol.* **14**, 199–224 (2000).

110. Mini, A., Palomba, D., Angrilli, A. & Bravi, S. Emotional information processing and visual evoked brain potentials. *Percept. Mot. Skills* **83**, 143–152 (1996).

111. Schupp, H. T., Cuthbert, B. N., Bradley, M. M., Birbaumer, N. & Lang, P. J. Probe P3 and blinks: two measures of affective startle modulation. *Psychophysiology* **34**, 1–6 (1997).

112. Palomba, D., Angrilli, A. & Mini, A. Visual evoked potentials, heart rate responses and memory to emotional pictorial stimuli. *Int. J. Psychophysiol.* **27**, 55–67 (1997).

113. Krolak-Salmon, P., Fischer, C., Vighetto, A. & Mauguière, F. Processing of facial emotional expression: spatio-temporal data as assessed by scalp event-related potentials. *Eur. J. Neurosci.* **13**, 987–994 (2001).

114. Schupp, H. *et al.* Brain processes in emotional perception: Motivated attention. *Cogn. Emot.* **18**, 593–611 (2004).

115. Olofsson, J. K., Nordin, S., Sequeira, H. & Polich, J. Affective picture processing: An integrative review of ERP findings. *Biol. Psychol.* **77**, 247–265 (2008).

116. Hajcak, G., MacNamara, A. & Olvet, D. M. Event-Related Potentials, Emotion, and Emotion Regulation: An Integrative Review. *Dev. Neuropsychol.* **35**, 129–155 (2010).

117. Wang, L., Sun, H., Li, L. & Meng, L. Hey, what is your choice? Uncertainty and inconsistency enhance subjective anticipation of upcoming information in a social context. *Exp. Brain Res.* **236**, 2797–2810 (2018).

118. Leng, Y. & Zhou, X. Interpersonal relationship modulates brain responses to outcome evaluation when gambling for/against others: An electrophysiological analysis. *Neuropsychologia* **63**, 205–214 (2014).

119. Cui, F., Zhu, X., Gu, R. & Luo, Y. When your pain signifies my gain: neural activity while evaluating outcomes based on another person's pain. *Sci. Rep.* **6**, 26426 (2016).

120. Wang, Y. *et al.* Psychophysiological correlates of interpersonal cooperation and aggression. *Biol. Psychol.* **93**, 386–391 (2013).

121. Wang, Y. *et al.* Social value orientation modulates the FRN and P300 in the chicken game. *Biol. Psychol.* **127**, 89–98 (2017).

122. Sun, L., Tan, P., Cheng, Y., Chen, J. & Qu, C. The effect of altruistic tendency on fairness in third-party punishment. *Front. Psychol.* **6**, (2015).

123. Boksem, M. A. S. & De Cremer, D. Fairness concerns predict medial frontal negativity amplitude in ultimatum bargaining. *Soc. Neurosci.* **5**, 118–128 (2010).

124. Qu, C., Wang, Y. & Huang, Y. Social exclusion modulates fairness consideration in the ultimatum game: an ERP study. *Front. Hum. Neurosci.* **7**, 505 (2013).

125. Massi, B. & Luhmann, C. C. Fairness influences early signatures of reward-related neural processing. *Cogn. Affect. Behav. Neurosci.* **15**, 768–775 (2015).

126. Fabre, E. F., Causse, M., Pesciarelli, F. & Cacciari, C. Sex and the money--How gender stereotypes modulate economic decision-making: An ERP study. *Neuropsychologia* **75**, 221–232 (2015).

127. Riepl, K., Mussel, P., Osinsky, R. & Hewig, J. Influences of State and Trait Affect on Behavior, Feedback-Related Negativity, and P3b in the Ultimatum Game. *PloS One* **11**, e0146358 (2016).

128. Nieuwenhuis, S. Learning, the P3, and the Locus Coeruleus-Norepinephrine System. in *Neural Basis of Motivational and Cognitive Control* (The MIT Press, 2011).

129. Aston-Jones, G. & Cohen, J. D. An Integrative Theory of Locus Coeruleus-Norepinephrine Function: Adaptive Gain and Optimal Performance. *Annu. Rev. Neurosci.* **28**, 403–450 (2005).

130. Trimber, E. M. & Luhmann, C. C. Implicit predictions of future rewards and their electrophysiological correlates. *Behav. Brain Res.* **333**, 184–191 (2017).

131. Pornpattananangkul, N. & Nusslock, R. Motivated to win: Relationship between anticipatory and outcome reward-related neural activity. *Brain Cogn.* **100**, 21–40 (2015).

132. Meyer, T. *et al.* The role of frontal EEG asymmetry in post-traumatic stress disorder. *Biol. Psychol.* **108**, 62–77 (2015).

133. Tulving, E., Kapur, S., Craik, F. I., Moscovitch, M. & Houle, S. Hemispheric encoding/retrieval asymmetry in episodic memory: positron emission tomography findings. *Proc. Natl. Acad. Sci. U. S. A.* **91**, 2016–2020 (1994).

134. Habib, R., Nyberg, L. & Tulving, E. Hemispheric asymmetries of memory: the HERA model revisited. *Trends Cogn. Sci.* **7**, 241–245 (2003).

135. Rossi, S. *et al.* Temporal Dynamics of Memory Trace Formation in the Human Prefrontal Cortex. *Cereb. Cortex* **21**, 368–373 (2011).

136. Cabeza, R. & Nyberg, L. Imaging cognition II: An empirical review of 275 PET and fMRI studies. *J. Cogn. Neurosci.* **12**, 1–47 (2000).

137. Zwissler, B. *et al.* Shaping Memory Accuracy by Left Prefrontal Transcranial Direct Current Stimulation. *J. Neurosci.* **34**, 4022–4026 (2014).

138. Murray, J. D., Jaramillo, J. & Wang, X.-J. Working Memory and Decision-Making in a Frontoparietal Circuit Model. *J. Neurosci.* **37**, 12167–12186 (2017).

139. Davidson, R. J. What does the prefrontal cortex 'do' in affect: perspectives on frontal EEG asymmetry research. *Biol. Psychol.* **67**, 219–233 (2004).

140. van Honk, J. & Schutter, D. J. L. G. From Affective Valence to Motivational Direction: The Frontal Asymmetry of Emotion Revised. *Psychol. Sci.* **17**, 963–965 (2006).

141. Harmon-Jones, E. & Gable, P. A. On the role of asymmetric frontal cortical activity in approach and withdrawal motivation: An updated review of the evidence. *Psychophysiology* **55**, (2018).

142. Rodrigues, J., Müller, M., Mühlberger, A. & Hewig, J. Mind the movement: Frontal asymmetry stands for behavioral motivation, bilateral frontal activation for behavior. *Psychophysiology* **55**, (2018).

143. Coan, J. A. & Allen, J. J. B. Frontal EEG asymmetry and the behavioral activation and inhibition systems. *Psychophysiology* **40**, 106–114 (2003).

144. Coan, J. A. & Allen, J. J. B. Frontal EEG asymmetry as a moderator and mediator of emotion. *Biol. Psychol.* **67**, 7–49 (2004).

145. Miller, A. & Tomarken, A. J. Task-dependent changes in frontal brain asymmetry: effects of incentive cues, outcome expectancies, and motor responses. *Psychophysiology* **38**, 500–511 (2001).

146. Pizzagalli, D. A., Sherwood, R. J., Henriques, J. B. & Davidson, R. J. Frontal brain asymmetry and reward responsiveness: a source-localization study. *Psychol. Sci.* **16**, 805–813 (2005).

147. Grimshaw, G. M. & Carmel, D. An asymmetric inhibition model of hemispheric differences in emotional processing. *Front. Psychol.* **5**, (2014).

148. Kelley, N. J., Hortensius, R., Schutter, D. J. L. G. & Harmon-Jones, E. The relationship of approach/avoidance motivation and asymmetric frontal cortical activity: A review of studies manipulating frontal asymmetry. *Int. J. Psychophysiol. Off. J. Int. Organ. Psychophysiol.* **119**, 19–30 (2017).

149. Berkman, E. T. & Lieberman, M. D. Approaching the Bad and Avoiding the Good: Lateral Prefrontal Cortical Asymmetry Distinguishes between Action and Valence. *J. Cogn. Neurosci.* **22**, 1970–1979 (2009).

150. Laufs, H. *et al.* EEG-correlated fMRI of human alpha activity. *NeuroImage* **19**, 1463–1476 (2003).

151. Reznik, S. J. & Allen, J. J. B. Frontal asymmetry as a mediator and moderator of emotion: An updated review. *Psychophysiology* **55**, (2018).

152. Balconi, M., Crivelli, D. & Vanutelli, M. E. Why to cooperate is better than to compete: brain and personality components. *BMC Neurosci.* **18**, 68 (2017).

153. Li, D. *et al.* Frontal Cortical Asymmetry May Partially Mediate the Influence of Social Power on Anger Expression. *Front. Psychol.* **7**, (2016).

154. Boksem, M. A. S., Smolders, R. & Cremer, D. D. Social power and approach-related neural activity. *Soc. Cogn. Affect. Neurosci.* **7**, 516–520 (2012).

155. Güntekin, B. & Başar, E. A review of brain oscillations in perception of faces and emotional pictures. *Neuropsychologia* **58**, 33–51 (2014).

156. Michel, C. M., Lehmann, D., Henggeler, B. & Brandeis, D. Localization of the sources of EEG delta, theta, alpha and beta frequency bands using the FFT dipole approximation. *Electroencephalogr. Clin. Neurophysiol.* **82**, 38–44 (1992).

157. Michel, C. M., Henggeler, B., Brandeis, D. & Lehmann, D. Localization of sources of brain alpha/theta/delta activity and the influence of the mode of spontaneous mentation. *Physiol. Meas.* **14 Suppl 4A**, A21-26 (1993).

158. Alper, K. R. *et al.* Correlation of PET and qEEG in normal subjects. *Psychiatry Res.* **146**, 271–282 (2006).

159. Mellem, M. S., Wohltjen, S., Gotts, S. J., Ghuman, A. S. & Martin, A. Intrinsic frequency biases and profiles across human cortex. *J. Neurophysiol.* **118**, 2853–2864 (2017).

160. Pripfl, J., Tomova, L., Riecansky, I. & Lamm, C. Transcranial Magnetic Stimulation of the Left Dorsolateral Prefrontal Cortex Decreases Cue-induced Nicotine Craving and EEG Delta Power. *Brain Stimulat.* **7**, 226–233 (2014).

161. Knyazev, G. G. Motivation, emotion, and their inhibitory control mirrored in brain oscillations. *Neurosci. Biobehav. Rev.* **31**, 377–395 (2007).

162. Knyazev, G. G. EEG delta oscillations as a correlate of basic homeostatic and motivational processes. *Neurosci. Biobehav. Rev.* **36**, 677–695 (2012).

163. Patron, E., Mennella, R., Messerotti Benvenuti, S. & Thayer, J. F. The frontal cortex is a heart-brake: Reduction in delta oscillations is associated with heart rate deceleration. *NeuroImage* **188**, 403–410 (2019).

164. Klados, M. A. *et al.* A framework combining delta Event-Related Oscillations (EROs) and Synchronisation Effects (ERD/ERS) to study emotional processing. *Comput. Intell. Neurosci.* 549419 (2009). doi:10.1155/2009/549419

165. Harmony, T. The functional significance of delta oscillations in cognitive processing. *Front. Integr. Neurosci.* **7**, (2013).

166. Huster, R. J., Enriquez-Geppert, S., Lavallee, C. F., Falkenstein, M. & Herrmann, C. S. Electroencephalography of response inhibition tasks: functional networks and cognitive contributions. *Int. J. Psychophysiol. Off. J. Int. Organ. Psychophysiol.* **87**, 217–233 (2013).

167. Nácher, V., Ledberg, A., Deco, G. & Romo, R. Coherent delta-band oscillations between cortical areas correlate with decision making. *Proc. Natl. Acad. Sci.* **110**, 15085–15090 (2013).

168. van de Vijver, I., van Driel, J., Hillebrand, A. & Cohen, M. X. Interactions between frontal and posterior oscillatory dynamics support adjustment of stimulus processing during reinforcement learning. *NeuroImage* **181**, 170–181 (2018).

169. Passecker, J. *et al.* Activity of Prefrontal Neurons Predict Future Choices during Gambling. *Neuron* **101**, 152-164.e7 (2019).

170. Dien, J. Looking both ways through time: the Janus model of lateralized cognition. *Brain Cogn.* **67**, 292–323 (2008).

171. Tops, M., Quirin, M., Boksem, M. A. S. & Koole, S. L. Large-scale neural networks and the lateralization of motivation and emotion. *Int. J. Psychophysiol. Off. J. Int. Organ. Psychophysiol.* **119**, 41–49 (2017).

172. Tremblay, L. & Schultz, W. Relative reward preference in primate orbitofrontal cortex. *Nature* **398**, 704–708 (1999).

173. Arana, F. S. *et al.* Dissociable contributions of the human amygdala and orbitofrontal cortex to incentive motivation and goal selection. *J. Neurosci. Off. J. Soc. Neurosci.* **23**, 9632–9638 (2003).

174. Padoa-Schioppa, C. & Assad, J. A. Neurons in the orbitofrontal cortex encode economic value. *Nature* **441**, 223 (2006).

175. Padoa-Schioppa, C. & Assad, J. A. The representation of economic value in the orbitofrontal cortex is invariant for changes of menu. *Nat. Neurosci.* **11**, 95–102 (2008).

176. Bzdok, D. *et al.* Segregation of the human medial prefrontal cortex in social cognition. *Front. Hum. Neurosci.* **7**, (2013).

177. Ochsner, K. N. *et al.* Reflecting upon feelings: an fMRI study of neural systems supporting the attribution of emotion to self and other. *J. Cogn. Neurosci.* **16**, 1746–1772 (2004).

178. Glimcher, P. Value-Based Decision Making. *Neuroeconomics Decis. Mak. Brain Second Ed.* 373–391 (2013). doi:10.1016/B978-0-12-416008-8.00020-6

179. Joiner, J., Piva, M., Turrin, C. & Chang, S. W. C. Social learning through prediction error in the brain. *NPJ Sci. Learn.* **2**, (2017).

180. Schurz, M., Radua, J., Aichhorn, M., Richlan, F. & Perner, J. Fractionating theory of mind: A meta-analysis of functional brain imaging studies. *Neurosci. Biobehav. Rev.* **42**, 9–34 (2014).

181. Behrens, T. E. J., Hunt, L. T., Woolrich, M. W. & Rushworth, M. F. S. Associative learning of social value. *Nature* **456**, 245–249 (2008).

182. Marek, S. & Dosenbach, N. U. F. The frontoparietal network: function, electrophysiology, and importance of individual precision mapping. *Dialogues Clin. Neurosci.* **20**, 133–140 (2018).

183. Wacongne, C. *et al.* Evidence for a hierarchy of predictions and prediction errors in human cortex. *Proc. Natl. Acad. Sci.* **108**, 20754–20759 (2011).

184. van den Berg, P. & Wenseleers, T. Uncertainty about social interactions leads to the evolution of social heuristics. *Nat. Commun.* **9**, 2151 (2018).

185. Strack, F. & Deutsch, R. The duality of everyday life: Dual-process and dual system models in social psychology. in *APA handbook of personality and social psychology, Volume 1: Attitudes and social cognition* 891–927 (American Psychological Association, 2015). doi:10.1037/14341-028

186. Suzuki, S. *et al.* Learning to simulate others' decisions. *Neuron* **74**, 1125–1137 (2012).

187. Friston, K. Learning and inference in the brain. *Neural Netw.* **16**, 1325–1352 (2003).

Supplementary material

Supplementary Video 1. Scalp topography dynamics of EEG during feedback processing at the iterated prisoner's dilemma. ERP grand average (*N*=30) with all outcomes types are included. A N1 followed by a P3 component is observed, at the end which a left-lateralized frontal component (termed 'LP') is sustained approximately until the end of the feedback presentation window. Time indicated in s. Colorbar units are in μV. Data as in Figure 1C (see main text).

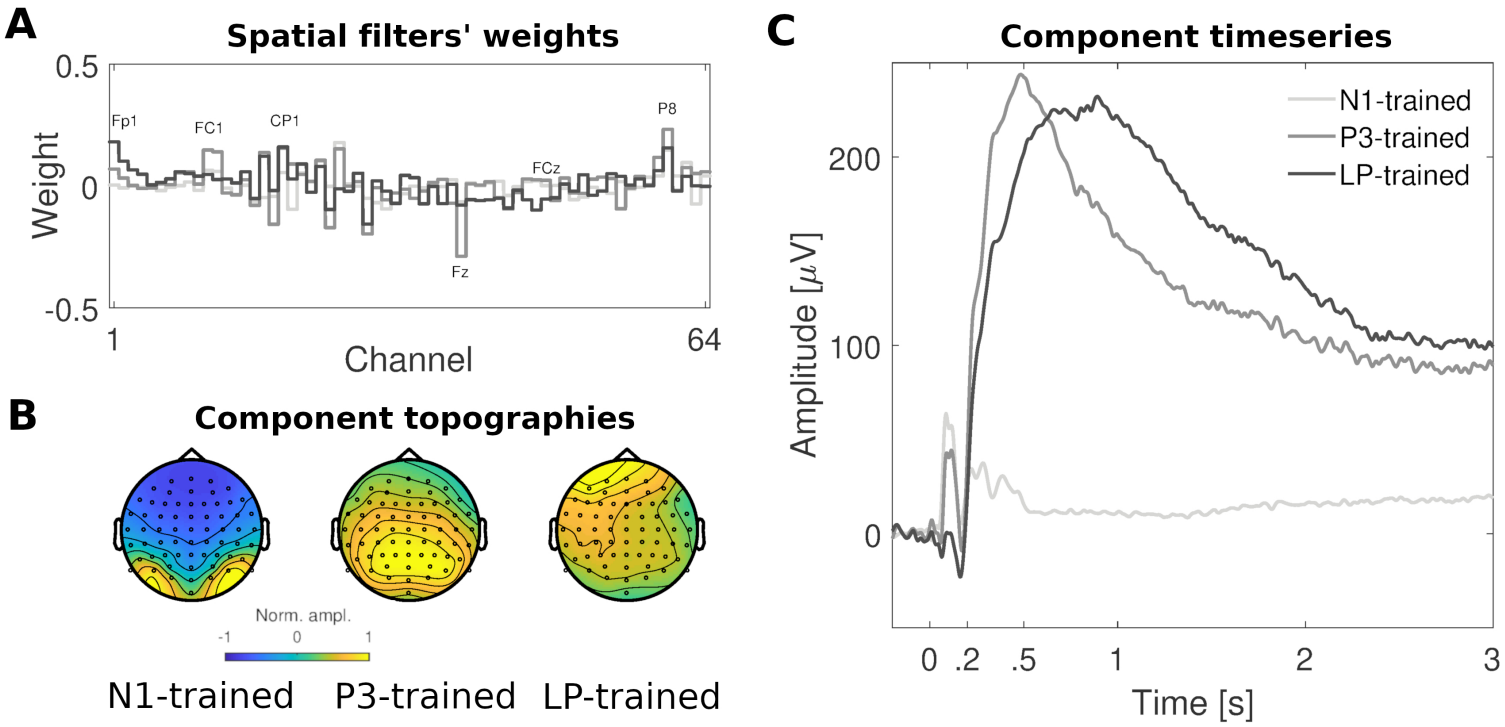

Supplementary Figure 1. Spatial filtering procedure. (A) Three spatial filters are separately trained on the basis of N1- (light), P3- (medium) or late potential-epochs (dark). Once estimated, each filter consists of a 64 array of linear coefficients designed to reveal specific components when applied to the whole EEG data. A selection of relevant sensors is shown. (B) Topography of the components associated with each spatial filter, and with reproducible activity across trials/participants. (C) Prisoner's dilemma feedback processing, with epochs shown averaged over outcomes post spatial filtering. Each waveform relates to a component and may be optimal for the respective temporal window from which it was estimated, but may further represent activity at other times.

Happiness

	CD	DC	DD
CC	<0.001	1	0.002
CD		<0.001	<0.001
DC			0.003

Anger

	CD	DC	DD
CC	<0.001	0.965	0.449
CD		<0.001	<0.001
DC			0.032

Sadness

	CD	DC	DD
CC	<0.001	0.017	0.223
CD		0.052	0.004
DC			1

Betrayal

	CD	DC	DD
CC	<0.001	1	0.052
CD		<0.001	0.001
DC			0.538

Guilt

	CD	DC	DD
CC	1	<0.001	0.545
CD		<0.001	1
DC			<0.001

Supplementary Table 1. Post-hoc multiple comparisons' significance tests for emotional scores. The p-values are indicated at each of the rated emotions, for each outcome type pair. CC outcomes are associated with happiness; CD outcomes with anger, sadness and betrayal; DC outcomes with hapiness and guilt (see Figure 1B).

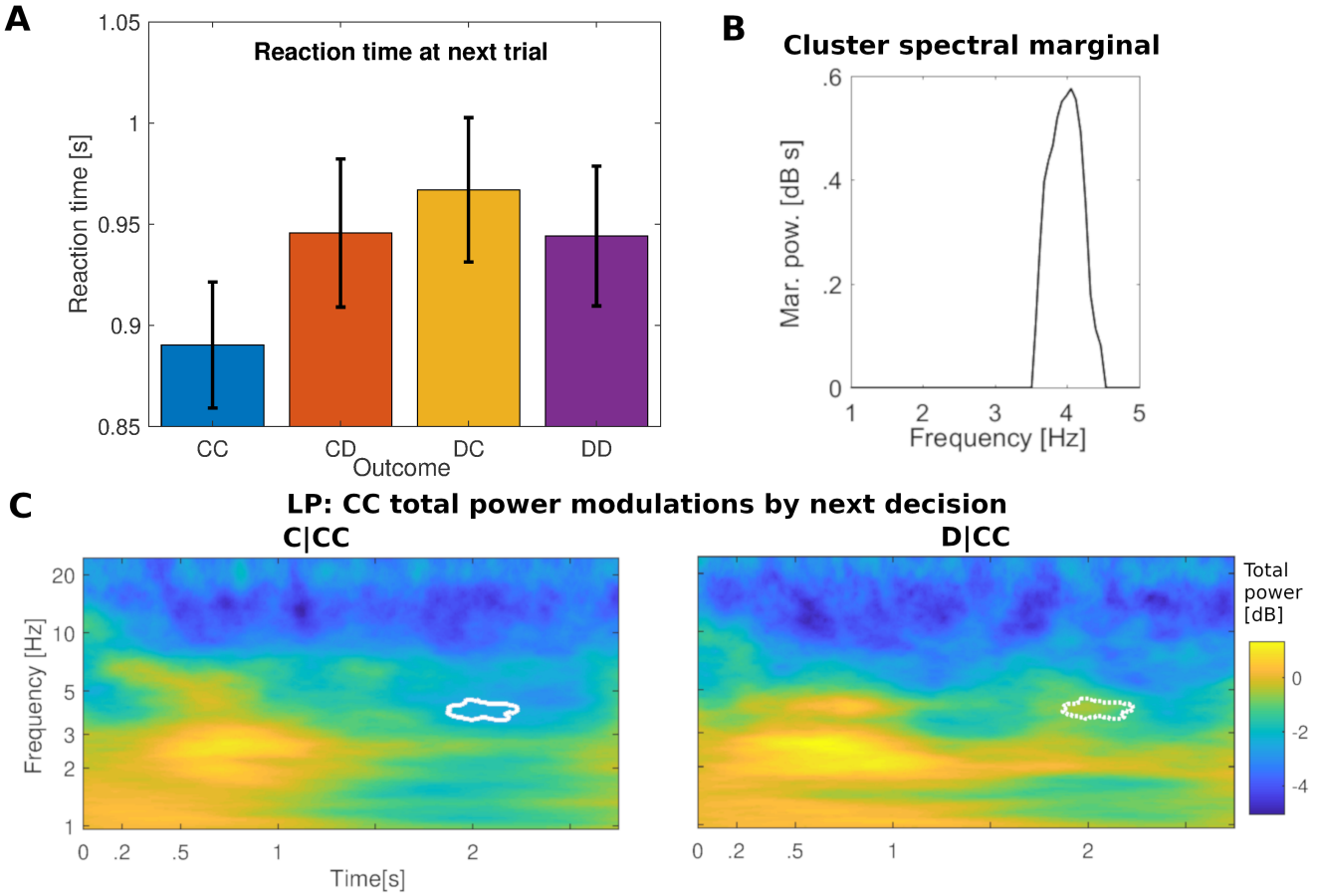

Supplementary Figure 2. (A) Grand average of next-round reaction times at the iPD are outcome-dependent. If the coplayer has chosen to cooperate, the player will at the next trial take less time to cooperate in turn than to defect. (B) The spectral profile of the significance cluster found for LP-delta activity at mutual cooperation trials, relating the player's next decision, is mainly centred on 4 Hz. (C) Total power correlograms from which the difference map was computed in (Fig. 4A), with cluster boundaries indicated, show different levels of baseline de-synchronization depending on the forthcoming cooperation decision, which are greater for mutual than unreciprocated cooperation.